Large deviations of spectral radius and "rightmost" particle for random matrices/charged fluids with logarithmic repulsion

Pierpaolo Vivo
*Department of Mathematics, King's College London, London WC2R 2LS, United Kingdom**

In these lecture notes I cover the material presented during my lectures at the Les Houches Summer School on "Theory of Large Deviations and Applications" held in July 2024.
[Please let me know of any typo/inaccuracy etc. that you may find in these notes, I will update them regularly before issuing the final version. The reference list is also largely incomplete and will be updated as well.]

* pierpaolo.vivo@kcl.ac.uk

CONTENTS

I. PROLOGUE

I wish to thank the organizers of the Les Houches Summer School on *Large deviations and applications* for inviting me, all the participants as well as my fellow lecturers. The material presented here is not new, I freely and liberally looted from published and unpublished material, of course giving credit to the original authors when needed. I leave some of the derivations as an exercise, and I strongly recommend that the interested reader attempt all exercises contained in these short notes.

II. TYPICAL VS. ATYPICAL FLUCTUATIONS: LARGE DEVIATIONS FOR COIN TOSSING

I will provide here a quick crash-course/appetizer on typical vs. atypical fluctuations and large deviations for those who have not met the concept and ideas before. I strongly recommend the review [1] by Hugo Touchette for a very thorough and enjoyable introduction to large deviations for physicists.

Consider the following question: what is the probability of getting M Heads out of N (fair) coin tosses? The exact formula for any M, N is given by the following binomial distribution

$$P(M,N) = \binom{N}{M}\frac{1}{2^N} \ , \tag{1}$$

where the binomial factor counts the number of possible arrangements of the M Heads within the sequence of N tosses. Clearly, we can now compute the average and variance of the number M of Heads as

$$\mu = \sum_{M=0}^{N} M\binom{N}{M}\frac{1}{2^N} = \frac{N}{2} \ , \tag{2}$$

$$\sigma^2 = \sum_{M=0}^{N} M^2\binom{N}{M}\frac{1}{2^N} - \mu^2 = \frac{N}{4} \ , \tag{3}$$

and appealing to Central Limit considerations, we expect that for large N the probability will converge to a Gaussian centred around μ and with fluctuations given by σ^2, i.e.

$$P(M,N) \to \frac{1}{\sqrt{\pi(N/2)}} \exp\left[-\frac{2}{N}\left(M-\frac{N}{2}\right)^2\right] . \tag{4}$$

On the other hand, it is easy to compute exactly the probability of an *anomalous event* characterised by *all* N tosses coming up Heads:

$$P(M=N,N) = \frac{1}{2^N} = \exp(-N\log 2) . \tag{5}$$

Comparing the two results for large N in (5) and (4) clearly shows that the two formulae are inconsistent for $M \simeq N$. In other word, the very natural Gaussian fluctuation law in Eq. (4) is only valid for *typical* fluctuations of the order of $\sim \sqrt{N}$ around the mean, but is inadequate to describe *large* (anomalous) fluctuations where M deviates from the average $N/2$ by an amount of order N.

Reconciling the two results requires introducing the *large deviation* (or rate) function, which governs the precise way the probability distribution decays when N is large, both in the vicinity and away from the most likely value. Take $P(M=Nx,N)$ for $0 \le x \le 1$ and expand the right hand side for large N using Stirling's formula for the factorials. Leaving the proof as an exercise, one obtains (neglecting pre-factors)

$$P(M=Nx,N) \approx \exp\left(-NI(x)\right) , \tag{6}$$

where

$$I(x) = x\log x + (1-x)\log(1-x) + \log 2 , \tag{7}$$

and the symbol $\approx$ stands for the precise asymptotics

$$\lim_{N\to\infty} \frac{-1}{N} \log P(M=Nx,N) = I(x) . \tag{8}$$

The rate function $I(x)$ is plotted in Fig. 1.

For $x \to 0$ (or $x \to 1$, symmetrically) the rate function converges to the value $\log 2$, which perfectly reproduces the exact result in Eq. (5). The rate function has a minimum (a zero) at $x = 1/2$, the "most likely" value (corresponding to $N/2$ Heads in N tosses), and then increases on either side of $x = 1/2$ leading $P(M = Nx, N)$ to correspondingly decay exponentially fast away from the most likely occurrence.

Interestingly enough, the rate function also provides important information about the *typical* fluctuations of the random variable M (= number of Heads) around its most likely value $M = N/2$. To see this, we can Taylor-expand $I(x)$ around $x = 1/2$ to get

$$I(x) = 2\left(x-\frac{1}{2}\right)^2 + \mathcal{O}\left(\left(x-\frac{1}{2}\right)^3\right) . \tag{9}$$

Inserting this quadratic behaviour back into Eq. (6) gives

$$P(M=Nx,N) \approx \exp\left(-2N\left(\frac{M}{N}-\frac{1}{2}\right)^2\right) = \exp\left(-\frac{2}{N}\left(M-\frac{N}{2}\right)^2\right) , \tag{10}$$

which precisely reproduces the Gaussian fluctuations of M around its mean value $N/2$ in Eq. (4).

The rate function $I(x)$ is therefore arguably a more fundamental and richer object than the Gaussian law (Eq. (4)), as it includes the latter but provides more accurate information about larger (anomalous) fluctuations much farther away from the mean value.

In these lectures, I will cover the explicit derivation of rate functions (using both rigorous and heuristic methods) for a richer class of random variables, which are not statistically independent.

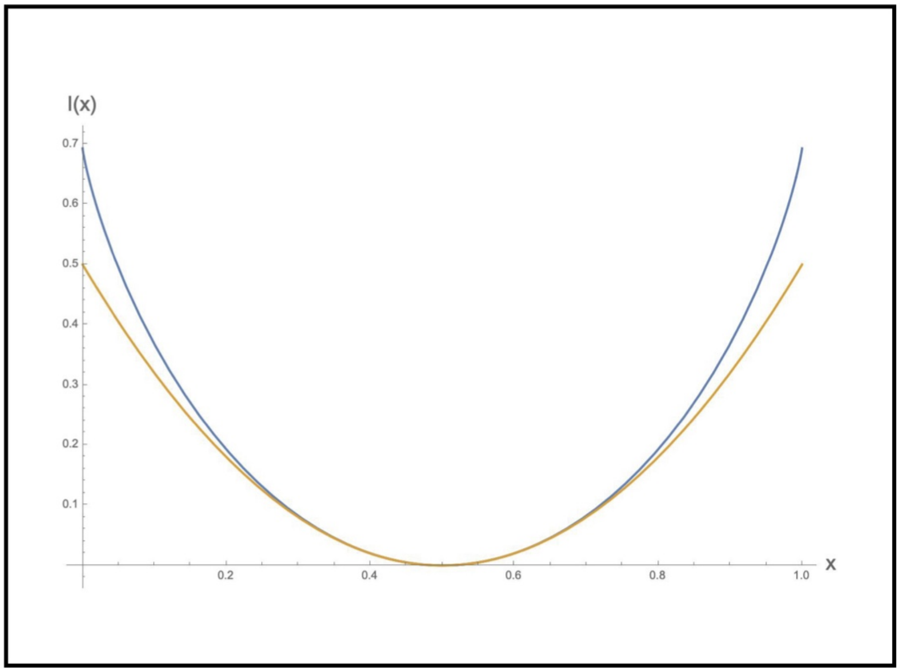

FIG. 1. Solid blue line: rate function $I(x)$ in Eq. (7). Solid yellow line: quadratic behaviour $2(x-1/2)^2$ around the minimum (see Eq. (9)). This plot – and the visible deviation between the two curves at the edges – clearly shows that the Gaussian behaviour around the minimum is inadequate to characterise anomalous events characterised by a very large or small number of Heads in a series of coin tosses.

III. GENERAL INTRODUCTION

In recent years there has been a considerable interest in the study of systems with logarithmic interactions. The simplest example of models in this class is the two-dimensional one-component plasma (2D-OCP). This system is also known in literature as 'jellium', 2D Dyson's gas or 2D Coulomb gas [2–9]. The 2D-OCP consists of N identical classical point-like particles, each carrying a charge q (one species of particle) on a two-dimensional domain. The Coulomb interaction between any two particles at distance $\vec{r}$ from each other is $-q^2 v(\vec{r})$, where $v(\vec{r})$ is the fundamental solution of the Poisson equation

$$\nabla^2 v(\vec{r}) = \delta(\vec{r}) \ . \tag{11}$$

In the planar case $v(\vec{r}) = (1/2\pi)\log(|\vec{r}|/L)$, where L is a length scale that fixes the zero of the potential. To ensure charge neutrality, the particles are embedded in a fixed neutralizing background with opposite charge $-qN$. The canonical distribution of the 2D-OCP at inverse temperature β is

$$\mathbb{P}_{\beta,N}\left(\vec{r}_1,\ldots,\vec{r}_N\right) = \frac{1}{\mathbb{Z}_{N,\beta}} \mathrm{e}^{-\beta E(\vec{r}_1,\ldots,\vec{r}_N)} \ , \tag{12}$$

$$E\left(\vec{r}_1,\ldots,\vec{r}_N\right) = -\frac{q^2}{2}\sum_{i\neq j}\log\left(\frac{|\vec{r}_i-\vec{r}_j|}{L}\right) + q^2 N \sum_k V\left(\frac{\vec{r}_k}{L}\right) \ . \tag{13}$$

In (13), $\vec{r}_i = (x_i, y_i) \in \mathbb{R}^2$ denotes the position of the i-th particle of the 2D-OCP ($i = 1,\ldots,N$) and $|\cdot|$ denotes the Euclidean distance. The first term in $E\left(\vec{r}_1,\ldots,\vec{r}_N\right)$ is the particle-particle contribution to the energy, while the second term is the particle-background contribution (the 2D-OCP experiences the electrostatic potential V generated by the fixed background). The coupling constant βq^2 is often referred to as *plasma parameter*.

This statistical mechanics fluid model has appeared in several areas of physics and mathematics. Indeed, the logarithmic repulsion in (13) does occur as interaction between vortices and dislocations in real systems such as superconductors [10], superfluids, rotating Bose-Einstein condensates [11–13] (we refer to [14] and [15] for detailed reviews). There is also a well-known analogy between the canonical measure (14) of the 2D-OCP and the Laughlin trial wave function [16] (in the symmetric gauge) in the theory of fractional quantum Hall effect [17]. In the large N limit with fixed potential (without the factor N in front of $V(\vec{r}/L)$), the 2D-OCP is equivalent to a class of growth models known as 'Laplacian growth' [9, 18].

In the following q and L will be set to one for simplicity. For notational convenience, we also identify $\mathbb{R}^2 \simeq \mathbb{C}$ and denote the positions of the particles in the plane by complex numbers $z_1, \ldots, z_N$. With these conventions, (12)-(13) read

$$\mathbb{P}_{\beta,N}\left(z_1,\ldots,z_N\right) = \frac{1}{\mathbb{Z}_{N,\beta}} \mathrm{e}^{-\beta E(z_1,\ldots,z_N)} \ , \tag{14}$$

$$E\left(z_1,\ldots,z_N\right) = -\frac{1}{2}\sum_{i\neq j}\log|z_i - z_j| + N\sum_k V\left(z_k\right) \ . \tag{15}$$

For $\beta = 2$ and 4, Eq. (14) turns out to coincide with the eigenvalues joint distribution for normal complex and normal self-dual matrix ensembles respectively [19–22].

Take for instance a $N \times N$ matrix whose entries are filled with independent (complex) Gaussian variables whose real and imaginary part have mean zero and variance $\sim 1/N$ (*complex Ginibre ensemble* [23]). The joint probability density that its N complex eigenvalues are found around the positions $\{z_1, \ldots, z_N\}$ in the complex plane is given by

$$\mathbb{P}_{\beta=2,N}\left(z_1,\ldots,z_N\right) = \frac{1}{\mathbb{Z}_{N,\beta=2}} \mathrm{e}^{-N\sum_k |z_k|^2} \prod_{j<k} |z_j - z_k|^2 \ , \tag{16}$$

which clearly coincides with (14) for $\beta = 2$ and $V(z) = |z|^2/2$. Note that – even if the entries are independent random variables – the eigenvalues are not due to the *Vandermonde determinant* term

$$\prod_{j>k}(z_j - z_k) = \det\begin{pmatrix} 1 & 1 & \cdots & 1 \\ z_1 & z_2 & \cdots & z_N \\ \vdots & \vdots & \ddots & \vdots \\ z_1^{N-1} & z_2^{N-1} & \cdots & z_N^{N-1} \end{pmatrix} \ , \tag{17}$$

which couples every particle (eigenvalues) with *all* the others. This is the price we pay for reducing the "complexity" of the matrix model from $\mathcal{O}(N^2)$ degrees of freedom (the entries) to $\mathcal{O}(N)$ degrees of freedom (the eigenvalues).

This means that, at inverse temperature $\beta = 2$, (14) is a *determinantal point process*. When the plasma particles experience a quadratic confinement $V(z) = |z|^2/2$ and for $\beta = 2$, the equilibrium density of the gas for large N is uniform in the unit disk[1] $D = \{|z| \leq R_\star = 1\}$ in the complex plane (*Girko-Ginibre circular law* [19]). The density and all correlation functions of the particles (eigenvalues) are also known for finite N due to the integrable determinantal structure of the joint distribution.

The circular law can be tested with the following code (see Fig. 2):

```
import numpy as np
import matplotlib.pyplot as plt
from scipy.linalg import eig

# Parameters
n = 1000
nsamples = 1

e = []

# Generating eigenvalues
for _ in range(nsamples):
    A = np.random.randn(n, n) + 1j * np.random.randn(n, n)
    eigenvalues = eig(A, right=False)
    e.extend(eigenvalues / np.sqrt(2 * n))
    e = np.array(e)

# Plotting eigenvalues
plt.plot(e.real, e.imag, 'or', label='Eigenvalues')
```

[1] Hereafter, we will denote by $R_\star$ the "upper edge" of the support of the equilibrium density of particles, i.e. the outer boundary beyond which particles cannot be found in the large N limit – both for the real and complex case.

```
# Plotting the unit circle
theta = np.linspace(0, 2 * np.pi, 1000)
plt.plot(np.cos(theta), np.sin(theta), label='Unit Circle')

plt.xlabel('Real Part')
plt.ylabel('Imaginary Part')
plt.title('Eigenvalues of Gaussian Non-Symmetric Matrices')
plt.legend()
plt.grid(True)
plt.axis('equal')
plt.show()
```

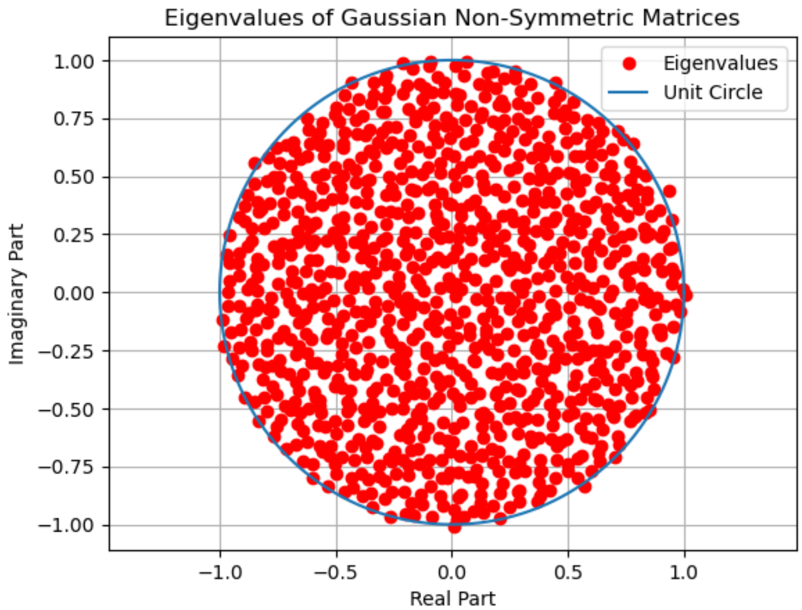

FIG. 2. Circular law for eigenvalues of Ginibre matrices.

In a completely analogous way, we can define a system of particles subject to logarithmic repulsion and confinement, but constrained to live on the real line. Using $\mathcal{P}$ instead of $\mathbb{P}$ to denote the joint distribution of the particle positions in this case, we have

$$\mathcal{P}_{\beta,N}\left(x_1,\ldots,x_N\right)=\frac{1}{\mathcal{Z}_{N,\beta}}\mathrm{e}^{-\beta E(x_1,\ldots,x_N)}\ , \tag{18}$$

$$E\left(x_1,\ldots,x_N\right)=-\frac{1}{2}\sum_{i\neq j}\log|x_i-x_j|+N\sum_k V\left(x_k\right)\ . \tag{19}$$

For $\beta=1,2,4$, Eq. (18) turns out to be the joint probability density of eigenvalues [24–26] of real symmetric, complex hermitian, and quaternion self-dual random matrices H respectively. Of particular importance are Gaussian random matrices, for which $V(x)=x^2/2$.

Depending on the physical symmetries, three classes of matrices with Gaussian entries arise: $(N\times N)$ real symmetric (Gaussian Orthogonal Ensemble (GOE)), $(N\times N)$ complex Hermitian (Gaussian Unitary Ensemble (GUE)) and $(2N\times 2N)$ self-dual Hermitian matrices (Gaussian Symplectic Ensemble (GSE)). In these models the probability distribution for the *entries* of a matrix H in the ensemble is given by

$$\mathcal{P}(H):=\mathcal{P}(H_{11},\ldots,H_{NN})\propto\exp\left(-\frac{\beta N}{2}(H,H)\right), \tag{20}$$

where (H,H) is the inner product on the space of matrices, invariant under orthogonal, unitary and symplectic transformations respectively and the parameter β is the Dyson index. In these three cases the inner products and the

Dyson indices are given by

$$(H,H) = \mathrm{Tr}(H^2); \quad \beta = 1 \qquad \text{GOE} \tag{21}$$
$$(H,H) = \mathrm{Tr}(H^* H); \quad \beta = 2 \qquad \text{GUE} \tag{22}$$
$$(H,H) = \mathrm{Tr}(H^\dagger H); \quad \beta = 4 \qquad \text{GSE} \tag{23}$$

where $\cdot^*$ denotes the hermitian conjugate of complex valued matrices and $\cdot^\dagger$ denotes the symplectic conjugate on quaternion-valued matrices. The above quadratic actions are the simplest forms (corresponding to free fields) of matrix models, which have been extensively studied in the context of particle physics and field theory.

A central result in the theory of Gaussian random matrices with real eigenvalues is the celebrated *Wigner semi-circle law*. It states that for large N and *on the average*, the N eigenvalues lie within a finite interval $\left[-\sqrt{2},\sqrt{2}\right]$, often referred to as the Wigner 'sea'. Within this sea, the average density of states has a semi-elliptical form that vanishes at the two edges $\pm R_\star = \pm\sqrt{2}$

$$\varrho_{\mathrm{sc}}(x) = \frac{1}{\pi}\left(R_\star^2 - x^2\right)^{1/2} . \tag{24}$$

The semicircle law (see Fig. 3 – analogous to the Girko-Ginibre law but for matrices with real spectrum – can be tested using the following code:

```python
import numpy as np
import matplotlib.pyplot as plt
from scipy.linalg import eigvalsh

# Parameters
n = 100
nsamples = 1000

e = []

# Generating eigenvalues
for _ in range(nsamples):
    A = np.random.randn(n, n) + 1j * np.random.randn(n, n)
    A = (A + A.T.conj()) / 2  # Making A Hermitian
    eigenvalues = eigvalsh(A)
    e.extend(eigenvalues / np.sqrt(2 * n))
    e = np.array(e)

# Function to normalize histogram
def normhist(vec, nbins):
    h, edges = np.histogram(vec, bins=nbins, density=True)
    ics = (edges[:-1] + edges[1:]) / 2
    return h, ics

# Plotting normalized histogram
hnorm, ics = normhist(e, 90)
plt.plot(ics, hnorm, 'or', label='Eigenvalue Distribution')

# Plotting the semicircle law
x = np.linspace(-np.sqrt(2), np.sqrt(2), 500)
y = (1 / np.pi) * np.sqrt(2 - np.round(x**2,4))
plt.plot(x, y, '-k', label='Semicircle Law')

plt.xlabel('Eigenvalue')
plt.ylabel('Density')
plt.title('Eigenvalue Distribution of Gaussian symmetric matrices and Semicircle Law')
plt.legend()
plt.grid(True)
plt.show()
```

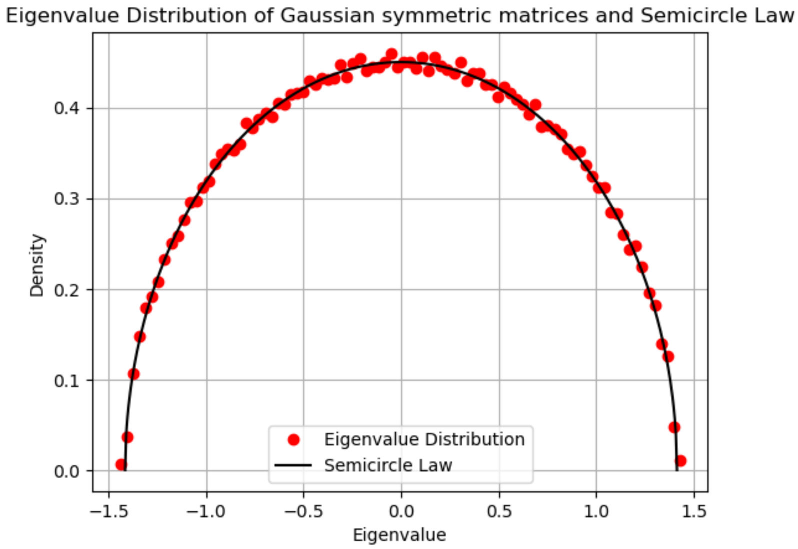

FIG. 3. Semicircle law for the average spectral density of eigenvalues in the Gaussian ensemble.

Mathematically, the average density of eigenvalues for finite N

$$\varrho_N(x) = \left\langle \frac{1}{N} \sum_{i=1}^{N} \delta(x - x_i) \right\rangle \tag{25}$$

provides the probability density of finding one eigenvalue around the position x (irrespective of which eigenvalue that is, and what the other eigenvalues are doing), where the average $\langle \cdot \rangle$ is taken w.r.t. the joint probability density of eigenvalues (18). Evaluating the average explicitly [26] yields to

$$\varrho_N(x) = \int \mathrm{d}x_2 \cdots \mathrm{d}x_N \mathcal{P}_{\beta,N}\left(x, \ldots, x_N\right) \ , \tag{26}$$

i.e. the average spectral density is the marginal of the joint density of eigenvalues. The semicircle law (24) is the limit

$$\varrho_{\mathrm{sc}}(x) = \lim_{N\to\infty} \varrho_N(x) \ . \tag{27}$$

For large N, it is therefore very difficult to find a Gaussian matrix with eigenvalues (suitably rescaled by $\sqrt{\beta N}$) larger than $\sqrt{2}$ or smaller than $-\sqrt{2}$. It is therefore natural to expect that the largest eigenvalue (or the rightmost charged particle) will be typically located around $\sqrt{2}$, with fluctuations that are interesting to characterize.

In these lectures, I will review results obtained for the following random variables

$$r_1 = \max_j x_j \qquad \text{(largest eigenvalue)} \tag{28}$$

$$r_2 = \max_j |x_j| \qquad \text{(spectral radius)} \ . \tag{29}$$

I will summarize both the typical fluctuations, and the large deviation regimes, characterizing probabilities that the "rightmost"/"outermost" particle is anomalously close to or far away from its typical location.

The plan of these lecture notes is as follows:

- In Lecture 1, I will discuss the special case of Gaussian ensembles and the distribution of the largest eigenvalue/rightmost particle of a log-gas in 1d, summarizing the Tracy-Widom law of typical fluctuations as well as the left and right large deviation functions describing anomalous fluctuations to the left and to the right, respectively, of the typical value. Following the approach by Majumdar and Vergassola [27, 28] (valid for all $\beta > 0$ and based on a physical argument), I will derive in detail the right large deviation function $\Phi_+(w)$ for $V(x) = x^2/2$, and will briefly comment on the different regimes for the fluctuations of r_2 for Gaussian non-hermitian matrices (log-gas in 2d).

- In Lectures 2/3, I will re-derive $\Phi_+(w)$ for $V(x) = x^2/2$ and $\beta = 1$ using a non-standard replica approach proposed in a more general context by Fyodorov and Le Doussal [29]. In this context, I will discuss an intriguing puzzle about the fact that only $\mathcal{O}(N)$ fluctuations can be recovered with this method (and not $\mathcal{O}(N^2)$ as well).

- In Lectures 4/5, I will instead focus on the spectral radius r_2 lifting the Gaussian assumptions, i.e. working with a more general confining potential $V(x)$ subject to some assumptions. For a general $V(x)$, $\mathrm{Prob}(\max_j |x_j| < R) \simeq \mathrm{e}^{-N^2 F(R)}$. Following the paper [30], I will show how to derive a general formula for the rate function $F(R)$, which can be interpreted as the *excess free energy* of a log-gas constrained within a box $[-R, R]$. From the general formula, I will derive as a general consequence that $F(R)$ displays a *third-order phase transition* at the critical value $R = R_\star$. I will also briefly discuss in class possible avenues for further research.

IV. LECTURE 1 - FLUCTUATIONS OF THE LARGEST EIGENVALUE OF GAUSSIAN ENSEMBLES AND RIGHT LARGE DEVIATION FUNCTION

In this section, I follow almost verbatim the insightful review [28] and the beautiful paper [31], which contains many interesting numerical tricks for the evaluation of Extreme Value distributions for random matrices.

Consider the joint probability density of eigenvalues for the Gaussian ensembles (18) with $V(x) = x^2/2$, and let $r_1 = \max_j x_j$ be the largest eigenvalue/position of the rightmost particle.

It turns out that as $N \to \infty$, defining

$$r_1 = \sqrt{2} + \frac{1}{\sqrt{2}} N^{-2/3} \chi_\beta \ , \tag{30}$$

the random variable χ_β is N-independent, and its Cumulative Distribution Function (CDF), $\mathcal{F}_\beta(x) = \mathrm{Prob}[\chi_\beta \leq x]$, is known as the β-Tracy-Widom (TW) distribution, known explicitly only for $\beta = 1, 2$ and 4. Tracy and Widom indeed obtained an explicit expression for $\beta = 2$ first [32] and subsequently for $\beta = 1$ and 4 [33] in terms of the Hastings-McLeod solution of the Painlevé II equation

$$q''(s) = 2q^3(s) + sq(s) \ , \ q(s) \sim \mathrm{Ai}(s) \ , \ s \to \infty \ , \tag{31}$$

with Airy function asymptotics as $s \to \infty$.

The CDF $\mathcal{F}_\beta(x)$ is then given explicitly for $\beta = 1$, 2 and 4 by [32, 33]

$$\begin{aligned}
\mathcal{F}_1(x) &= \exp\left[-\frac{1}{2}\int_x^\infty \left[(s-x)q^2(s) + q(s)\right] \mathrm{d}s\right] , \\
\mathcal{F}_2(x) &= \exp\left[-\int_x^\infty (s-x)q^2(s)\,\mathrm{d}s\right] , \\
\mathcal{F}_4(2^{-\frac{2}{3}}x) &= \exp\left[-\frac{1}{2}\int_x^\infty (s-x)q^2(s)\,\mathrm{d}s\right] \cosh\left[\frac{1}{2}\int_x^\infty q(s)\,\mathrm{d}s\right] .
\end{aligned} \tag{32}$$

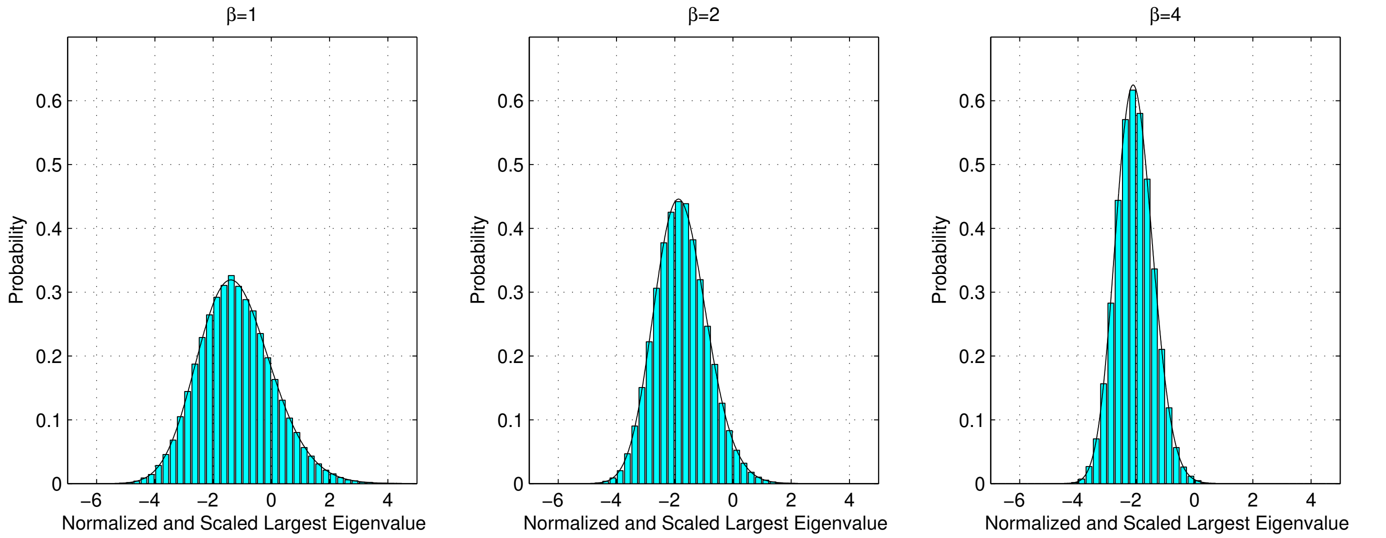

FIG. 4. Probability distribution of scaled largest eigenvalue χ_β (10^5 repetitions, $N = 10^9$). Solid lines are the Tracy-Widom probability densities (derivatives of Eqs. (32)). Plots and algorithm for fast evaluation taken from [31] – also reproduced at the end of this section.

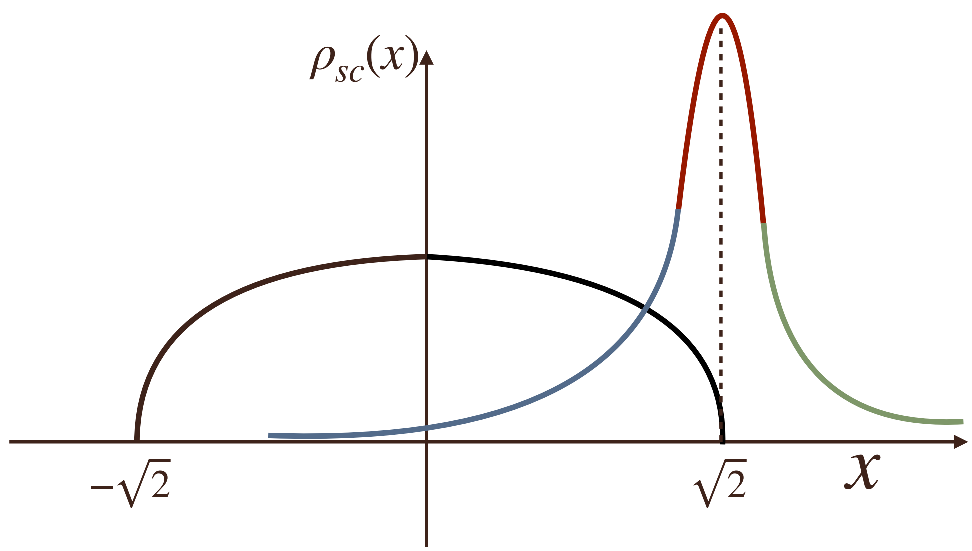

FIG. 5. Sketch of the different regimes for the fluctuations of the largest eigenvalue r_1 of Gaussian ensembles. In Red, the regime of typical fluctuations on a narrow scale of $\sim \mathcal{O}(N^{-2/3})$ around its mean $\langle r_1 \rangle = \sqrt{2}$. In Blue, the left large deviations. In Green, the right large deviations.

For other values of β it can be shown that χ_β describes the fluctuations of the ground state of the following one-dimensional Schrödinger operator, called the "stochastic Airy operator" [34, 35]

$$\mathcal{H}_\beta = -\frac{\mathrm{d}^2}{\mathrm{d}x^2} + x + \frac{2}{\sqrt{\beta}}\eta(x) \; , \tag{33}$$

where $\eta(x)$ is Gaussian white noise, of zero mean and with delta correlations, $\overline{\eta(x)\eta(x')} = \delta(x - x')$. For arbitrary

$\beta > 0$, the CDF $\mathcal{F}_\beta(x)$, or equivalently the PDF $\mathcal{F}'_\beta(x)$ of χ_β has rather asymmetric non-Gaussian tails,

$$\mathcal{F}'_\beta(x) \approx \begin{cases} \exp\left[-\dfrac{\beta}{24}|x|^3\right], \ x \to -\infty \\ \\ \exp\left[-\dfrac{2\beta}{3}x^{3/2}\right], \ x \to +\infty , \end{cases} \tag{34}$$

where $\approx$ stands for a logarithmic equivalent.

These TW distributions also describe the top eigenvalue statistics of large real [36, 37] and complex [38] Gaussian covariance matrices. Amazingly, the same TW distributions have emerged in a number of a priori unrelated problems [39] such as the longest increasing subsequence of random permutations [40], directed polymers [38, 41] and growth models [42] in the Kardar-Parisi-Zhang (KPZ) universality class in $(1 + 1)$ dimensions as well as for the continuum $(1+1)$-dimensional KPZ equation [43–46], sequence alignment problems [47], mesoscopic fluctuations in quantum dots [48], height fluctuations of non-intersecting Brownian motions over a fixed time interval [49, 50], height fluctuations of non-intersecting interfaces in presence of a long-range interaction induced by a substrate [51], and also in finance [52]. Remarkably, the TW distributions have been recently observed in experiments on nematic liquid crystals [53] (for $\beta = 1, 2$) and in experiments involving coupled fiber lasers [54] (for $\beta = 1$).

While the TW density describes the probability of *typical* fluctuations of r_1 around its mean $\langle r_1\rangle = \sqrt{2}$ on a *small* scale[2] of $\sim \mathcal{O}(N^{-2/3})$, it does not describe *atypically* large fluctuations, e.g., of order $\mathcal{O}(1)$ around its mean (see Fig. 5 for a sketch). The probability of atypically large fluctuations, to leading order for large N, is described by two large deviations (or rate) functions $\Phi_-(w)$ (for fluctuations to the *left* of the mean) and $\Phi_+(w)$ (for fluctuations to the *right* of the mean). More precisely, the behavior of the CDF $F_N(w) = \mathrm{Prob}[r_1 \le w]$ of r_1 for large but finite N is described as follows

$$F_N(w) \approx \begin{cases} \exp\left[-\beta N^2 \Phi_-(w)\right] & , \ w < \sqrt{2} \ \& \ |w-\sqrt{2}| \sim \mathcal{O}(1) \\ \\ \mathcal{F}_\beta\left(\sqrt{2}N^{\frac{2}{3}}(w-\sqrt{2})\right) & , \ |w-\sqrt{2}| \sim \mathcal{O}(N^{-\frac{2}{3}}) \\ \\ 1-\exp\left[-\beta N \Phi_+(w)\right] & , \ w > \sqrt{2} \ \& \ |w-\sqrt{2}| \sim \mathcal{O}(1) \ . \end{cases} \tag{37}$$

Equivalently, the PDF $f_{r_1}(w)$ of r_1, obtained from the derivative $f_{r_1}(w) = \mathrm{d}F_N(w)/\mathrm{d}w$ reads (keeping only leading order terms for large N)

$$f_{r_1}(w) = \mathcal{P}(r_1 = w, N) \approx \begin{cases} \exp\left[-\beta N^2 \Phi_-(w)\right] & , \ w < \sqrt{2} \ \& \ |w-\sqrt{2}| \sim \mathcal{O}(1) \\ \\ \sqrt{2}N^{\frac{2}{3}}\mathcal{F}'_\beta\left(\sqrt{2}N^{\frac{2}{3}}(w-\sqrt{2})\right) & , \ |w-\sqrt{2}| \sim \mathcal{O}(N^{-\frac{2}{3}}) \\ \\ \exp\left[-\beta N \Phi_+(w)\right] & , \ w > \sqrt{2} \ \& \ |w-\sqrt{2}| \sim \mathcal{O}(1) \ . \end{cases} \tag{38}$$

The physical mechanisms responsible for the left and right large deviation tails are very different, which is reflected in the different *speeds* of the large deviations, N^2 vs. N. Physically, having the rightmost charged particle anomalously dislodged to the left side requires a global rearrangement of all other mutually repelling charges, which are "squeezed" into an unnatural and much less comfortable configuration. The all-to-all cooperation among the N charges necessary to achieve the relocation of r_1 is signalled by the $\sim N^2$ speed of the left rate function. On the contrary, the rightmost charge can take up an anomalous location to the right of its typical value without significantly disturbing the other $N-1$ charges. The physical intuition here leads to the calculation I present in the next section. It is therefore comparatively much easier to have r_1 much larger than its typical value than having it much smaller than its typical value. We will refer to the two situations as *pushed* Coulomb gas or *pulled* Coulomb gas respectively.

---

[2] The scale $N^{-2/3}$ of typical fluctuations can be determined by a heuristic scaling argument. To estimate the typical scale δr_1 of the fluctuations of r_1, one can apply a standard criterion of Extreme Value Statistics, i.e.

$$\int_{\sqrt{2}-\delta r_1}^{\sqrt{2}} \varrho_{\mathrm{sc}}(x)\mathrm{d}x \sim \frac{1}{N} , \tag{35}$$

which simply states that the fraction of eigenvalues to the right of the maximum (including itself) must be typically $1/N$. Using the asymptotic behavior near the upper edge $R_\star = \sqrt{2}$, $\varrho_{\mathrm{sc}}(x) \propto (\sqrt{2}-x)^{1/2}$ as $x \to \sqrt{2}$, one obtains (exercise) [55, 56]

$$\delta r_1 = \sqrt{2} - r_1 = \mathcal{O}(N^{-2/3}) . \tag{36}$$

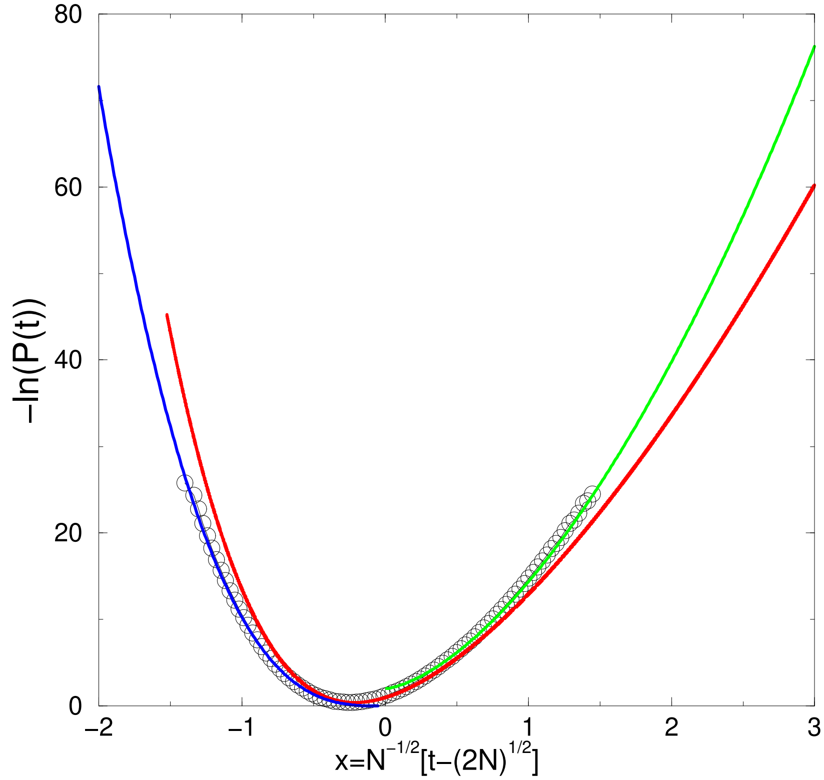

FIG. 6. Numerical results for the maximum eigenvalue distribution (circles) for $N = 10$ real ($\beta = 1$) Gaussian matrices, compared with the Tracy-Widom result (red line) and the exact right (green line) and left (blue line) large deviation functions. Figure taken from [27].

Note that while the TW distribution $\mathcal{F}_\beta(x)$, describing the central part of the probability distribution of r_1, depends explicitly on β [see Eq. (32)], the two leading order rate functions $\Phi_\mp(w)$ are independent of β. Exploiting a simple physical method based on the Coulomb gas, the left rate function $\Phi_-(z)$ was first explicitly computed in [57, 58]

$$\Phi_-(w) = \frac{1}{108}\Big[36w^2 - w^4 - (15w + w^3)\sqrt{w^2+6} + 27\left(\log 18 - 2\log\left(w + \sqrt{w^2+6}\right)\right)\Big] \;,\; w < \sqrt{2}\,. \tag{39}$$

Note in particular the behavior when w approaches the critical point $R_\star = \sqrt{2}$ from below[3]

$$\Phi_-(w) \sim \frac{1}{6\sqrt{2}}(\sqrt{2} - w)^3 \;,\; w \to \sqrt{2}\,. \tag{40}$$

On the other hand, the right rate function $\Phi_+(w)$ was computed in [27]. A more complicated, albeit mathematically rigorous, derivation (but only valid for $\beta = 1$) of $\Phi_+(w)$ in the context of spin glass models can be found in [59]. Incidentally, the right tail of x_1 can also be directly related to the finite N behavior of the average density of states to the right of the Wigner sea [60]. Indeed, for $\beta = 1$, this finite N right tail of the density was computed in Ref. [61], from which one can extract the right rate function $\Phi_+(w)$. It reads

$$\Phi_+(w) = \frac{1}{2}w\sqrt{w^2-2} + \log\left[\frac{w - \sqrt{w^2-2}}{\sqrt{2}}\right] , \tag{41}$$

[3] The exponent 3 is the signature of an underlying third-order phase transition in the associated Coulomb gas, see [28] for details. I will come back to this point when discussing the fluctuations of the spectral radius in Section VI.

with the asymptotic behavior

$$\Phi_+(w) \sim \frac{2^{7/4}}{3}(w-\sqrt{2})^{3/2}\ ,\ w\to\sqrt{2}\ . \tag{42}$$

Interestingly, one can show that the central (typical) fluctuations, described by the Tracy-Widom law, match smoothly with the behavior of the rate functions $\Phi_\pm(x)$ when $x \to R_\star = \sqrt{2}$, according to the principle *The most unlikely of typical fluctuations should smoothly match the most likely of atypical fluctuations.*

To see this, let us first consider the left tail in (38), i .e. when $w < R_\star = \sqrt{2}$. When $w \to R_\star = \sqrt{2}$ from below we can substitute the asymptotic behavior of the rate function $\Phi_-(w)$ from (40) in the first line of (38). This yields for $1 \ll \sqrt{2} - w \ll \sqrt{2}$

$$f_{r_1}(w) = \mathcal{P}(r_1 = w, N) = \frac{\mathrm{d}}{\mathrm{d}w}F_N(w) \approx \quad \exp\left(-\frac{\beta}{6\sqrt{2}}N^2(\sqrt{2}-w)^3\right)\ . \tag{43}$$

On the other hand, consider now the second line of (38) that describes the central typical fluctuations. When the deviation from the typical value $R_\star = \sqrt{2}$ is large ($\sqrt{2} - w \sim \mathcal{O}(1)$) we can substitute in the second line of (38) the left tail asymptotic behavior of the β-Tracy-Widom distribution (34) giving

$$f_{r_1}(w) = \mathcal{P}(r_1 = w, N) = \frac{\mathrm{d}}{\mathrm{d}w}F_N(w) \approx \exp\left[-\frac{\beta}{24}\left[2^{1/2}N^{2/3}(\sqrt{2}-w)\right]^3\right]\ , \tag{44}$$

which after a trivial rearrangement, is identical to (43). This shows that the left tail of the central region matches smoothly with the left large deviation function. Similarly, on the right side, using the behavior of $\Phi_+(x)$ in (42), one finds from (38) that

$$f_{r_1}(w) = \mathcal{P}(r_1 = w, N) = \frac{\mathrm{d}}{\mathrm{d}w}F_N(w) \approx \exp\left(-\frac{2^{7/4}\beta}{3}N(w-\sqrt{2})^{3/2}\right)\ , \tag{45}$$

for $1 \ll w - \sqrt{2} \ll \sqrt{2}$, which matches with the right tail of the central part described by $\mathcal{F}'_\beta(x)$ (34). Such a mechanism of matching between the central part and the large deviation tails of the distribution have been found in other similar problems [27, 62] (see also Appendix IV C for a counter-example).

I will reproduce in the next subsection the main steps of the derivation of $\Phi_+(w)$.

A. Derivation of right deviation tail using Coulomb gas method

Following [27], the correct strategy to extract the right large deviation tail turns out to consider directly the probability density function of r_1, rather than its Cumulative Distribution Function $F_N(w)$ given by

$$F_N(w) = \mathrm{Prob}[r_1 \le w] = \mathrm{Prob}[x_1 \le w, \ldots, x_N \le w] = \frac{\int_{-\infty}^{w}\cdots\int_{-\infty}^{w}\mathrm{d}x_1\cdots\mathrm{d}x_N\ \mathrm{e}^{-\beta E(x_1,\ldots,x_N)}}{\int_{-\infty}^{\infty}\cdots\int_{-\infty}^{\infty}\mathrm{d}x_1\cdots\mathrm{d}x_N\ \mathrm{e}^{-\beta E(x_1,\ldots,x_N)}}\ , \tag{46}$$

with

$$E(x_1,\ldots,x_N) = \frac{N}{2}\sum_{k=1}^{N}x_k^2 - \frac{1}{2}\sum_{i\neq j}\log|x_i - x_j|\ . \tag{47}$$

Taking derivative of (46) with respect to w and using the fact that the integrand is a symmetric function[4] in the variables $(x_1,\ldots,x_N)$ yields an exact expression (ignoring proportionality constants) for the probability density function of r_1,

$$f_{r_1}(w) = \mathcal{P}(r_1 = w, N) \propto \mathrm{e}^{-N\beta\frac{w^2}{2}}\int_{-\infty}^{w}\mathrm{d}x_1\cdots\int_{-\infty}^{w}\mathrm{d}x_{N-1}\ \mathrm{e}^{\beta\sum_{j=1}^{N-1}\log(|w-x_j|)}\mathcal{P}_{\beta,N-1}(x_1,\ldots,x_{N-1})\ , \tag{48}$$

[4] Take $N = 2$. The derivative $\partial_w \int_{-\infty}^{w}\int_{-\infty}^{w} f(x_1,x_2)\mathrm{d}x_1\mathrm{d}x_2 = \int_{-\infty}^{w}\mathrm{d}x_2 f(w,x_2) + \int_{-\infty}^{w}\mathrm{d}x_1 f(x_1,w) = 2\int_{-\infty}^{w}\mathrm{d}x_1 f(x_1,w)$ using $f(x_1,x_2) = f(x_2,x_1)$.

where $\mathcal{P}_{\beta,N-1}(x_1,\cdots,x_{N-1})$ is the joint probability density given in (18) for $(N-1)$ eigenvalues and the energy function given in (47).

Having a fixed charge located at $w-\sqrt{2}\sim\mathcal{O}(1)$ (i.e. far away to the right of all other charges) should not disturb (to leading order) the equilibrium configuration of the remaining $N-1$ charges. Therefore, we can formally replace $\mathcal{P}_{\beta,N-1}(x_1,\cdots,x_{N-1})$ in the integral (48) with $\prod_{j=1}^{N-1}\delta(x_j-x_j^\star)$, where $x_j^\star$ are the most probable equilibrium locations the other charges are pinned to.

This way we obtain

$$\mathcal{P}(r_1=w,N)\propto \mathrm{e}^{-N\beta\frac{w^2}{2}+\beta\sum_{j=1}^{N-1}\log(|w-x_j^\star|)} \tag{49}$$

which can be further approximated by

$$\mathcal{P}(r_1=w,N)\propto \exp\left[-\beta N\frac{w^2}{2}+\beta N\int\log|w-x|\,\varrho_{\mathrm{sc}}(x)\,\mathrm{d}x\right] . \tag{50}$$

In (50), we have converted the sum into an integral, and used the fact that the probability density of the equilibrium locations of a an eigenvalue in the unperturbed Gaussian ensemble is given by the semicircle law (24).

Thus, one gets to leading order for large N [27]

$$\mathcal{P}(r_1=w,N)\sim\exp\left[-\beta N\Phi_+(w)\right] , \tag{51}$$

where the right rate function $\Phi_+(w)$ is given by (restoring an overall normalization constant)

$$\boxed{\Phi_+(w)=\frac{w^2}{2}-\int_{-\sqrt{2}}^{\sqrt{2}}\log\left(w-x\right)\varrho_{\mathrm{sc}}(x)\mathrm{d}x+A\ ,\qquad w>\sqrt{2}} \tag{52}$$

where the constant A is fixed such that $\Phi_+(w=\sqrt{2})=0$, since our reference configuration is the one where typically $r_1=\sqrt{2}$, and $\varrho_{\mathrm{sc}}(x)=\frac{1}{\pi}\sqrt{2-x^2}$. Evaluating the integral in (52), one obtains the result for $\Phi_+(w)$ given in (41), as I now show.

1. *Computing the integral in* (52)

Let us consider the integral appearing in (52) for $w>\sqrt{2}$

$$\frac{1}{\pi}\int_{-\sqrt{2}}^{+\sqrt{2}}\mathrm{d}x\log\left(w-x\right)\sqrt{2-x^2}\equiv I(w) . \tag{53}$$

We may rewrite the log term as follows

$$\log\left(w-x\right)=\log(w)+\log\left(1-\frac{x}{w}\right)=\log(w)-\sum_{n=1}^{\infty}\frac{1}{n}\frac{x^n}{w^n} . \tag{54}$$

The integral therefore becomes

$$I(w)=\frac{1}{\pi}\left[\log(w)\int_{-\sqrt{2}}^{+\sqrt{2}}\mathrm{d}x\sqrt{2-x^2}-\sum_{n=1}^{\infty}\frac{1}{n}\frac{1}{w^n}C_n\right] . \tag{55}$$

with $C_n=\int_{-\sqrt{2}}^{+\sqrt{2}}\mathrm{d}x\ x^n\sqrt{2-x^2}$. Setting $x=\sqrt{2}t$ we obtain

$$\begin{aligned}C_n&=\sqrt{2}\sqrt{2}(\sqrt{2})^n\int_{-1}^{1}\mathrm{d}t\ t^n\sqrt{1-t^2}\\&=(\sqrt{2})^n\frac{\left[1+(-1)^n\right]\sqrt{\pi}\ \Gamma\left(\frac{n+1}{2}\right)}{2\Gamma\left(2+\frac{n}{2}\right)} .\end{aligned} \tag{56}$$

From the definition of C_n we note that the integral is correctly non-zero only if n is even. Therefore, we set $n = 2k$, thus obtaining

$$-\sum_{n=1}^{\infty}\frac{1}{n}\frac{1}{w^n}C_n = -\frac{\sqrt{\pi}}{2}\sum_{k=1}^{\infty}\frac{\Gamma\left(k+\frac{1}{2}\right)}{\Gamma\left(k+2\right)}\frac{1}{k}\left(\frac{2}{w^2}\right)^k = -\frac{\sqrt{\pi}}{2}\frac{2}{w^2}\sum_{k=0}^{\infty}\frac{\Gamma\left(k+\frac{3}{2}\right)}{\Gamma\left(k+3\right)}\frac{1}{k+1}\left(\frac{2}{w^2}\right)^k . \tag{57}$$

We may now appeal to the definition of the generalized hypergeometric function ${}_pF_q$

$${}_pF_q(\{a_1,\dots,a_p\};\{b_1,\dots,b_q\};z) = \sum_{k=0}^{\infty}\frac{\prod_{j=1}^{p}(a_j)_k}{\prod_{j=1}^{q}(b_j)_k}\frac{z^k}{k!} , \tag{58}$$

with $(\gamma)_k = \Gamma(\gamma+k)/\Gamma(\gamma)$ being the Pochhammer symbol, and note the identity

$$\frac{\frac{\Gamma(1+k)}{\Gamma(1)}\frac{\Gamma(1+k)}{\Gamma(1)}\frac{\Gamma(3/2+k)}{\Gamma(3/2)}}{\frac{\Gamma(2+k)}{\Gamma(2)}\frac{\Gamma(3+k)}{\Gamma(3)}} = \frac{4\Gamma\left(k+\frac{3}{2}\right)}{\sqrt{\pi}(k+1)\Gamma(k+3)} \tag{59}$$

to be able to re-cast Eq. (57) as

$$-\sum_{n=1}^{\infty}\frac{1}{n}\frac{1}{w^n}C_n = -\frac{\sqrt{\pi}}{2}\frac{2}{w^2}\frac{\sqrt{\pi}}{4}\,{}_3F_2\left(\left\{1,1,\frac{3}{2}\right\};\{2,3\};\frac{2}{w^2}\right) . \tag{60}$$

For these special values of its parameters, the generalized hypergeometric function ${}_3F_2\left(\{1,1,\frac{3}{2}\};\{2,3\};z\right)$ has a representation in terms of elementary functions [63]

$${}_3F_2\left(\left\{1,1,\frac{3}{2}\right\};\{2,3\};z\right) = \frac{4}{z^2}\left[-2\log\left(\frac{1+\sqrt{1-z}}{2}\right)z + z + 2\sqrt{1-z} - 2\right] . \tag{61}$$

Combining everything together, we get

$$I(w) = \log w - \frac{w^2}{4}\left[-\frac{4}{w^2}\log\left(\frac{w+\sqrt{w^2-2}}{2w}\right) + \frac{2}{w^2} + \frac{2}{w}\sqrt{w^2-2} - 2\right] \tag{62}$$

$$= \log w + \log\left(\frac{w+\sqrt{w^2-2}}{2w}\right) - \frac{1}{2} - \frac{w}{2}\sqrt{w^2-2} + \frac{w^2}{2} . \tag{63}$$

2. Calculation of the full rate function $\Phi_+(w)$

The result obtained for $I(w)$ can be now inserted in Eq. (52). First, we compute the constant A by setting:

$$\Phi_+(\sqrt{2}) = \frac{(\sqrt{2})^2}{2} - \log\sqrt{2} - \log\left(\frac{\sqrt{2}}{2\sqrt{2}}\right) + \frac{1}{2} - \frac{(\sqrt{2})^2}{2} + A = 0 \Rightarrow A = -\frac{1}{2} - \frac{1}{2}\log 2 . \tag{64}$$

Then, we obtain

$$\Phi_+(w) = \frac{w^2}{2} - \log w - \log\left(\frac{w+\sqrt{w^2-2}}{2w}\right) + \frac{1}{2} + \frac{w}{2}\sqrt{w^2-2} - \frac{w^2}{2} - \frac{1}{2} - \frac{1}{2}\log 2$$

$$= \frac{1}{2}w\sqrt{w^2-2} - \log\left(\frac{w+\sqrt{w^2-2}}{\sqrt{2}}\right) . \tag{65}$$

Finally, multiplying and dividing by $w - \sqrt{w^2-2}$ inside the logarithm gives the expression in Eq. (41)

$$\boxed{\Phi_+(w) = \frac{1}{2}w\sqrt{w^2-2} + \log\left(\frac{w-\sqrt{w^2-2}}{\sqrt{2}}\right) .} \tag{66}$$

To compute the higher order corrections to the right tail one needs more sophisticated techniques. These were obtained in [64] for $\beta = 2$, using a method based on orthogonal polynomials over the unusual interval $(-\infty, w]$ and adapting a technique originally developed in the context of QCD [65]. The right large deviation behavior of r_1 has been computed to all orders in N by a generalized loop equation method by Borot and Nadal [66] (see also Ref. [60]). Finally, the unusual orthogonal polynomial method developed in Ref. [64] has been extended and generalized to matrix models with higher order critical points [67, 68].

The topic of large deviations for extreme eigenvalues (and empirical spectral measure more generally) has never ceased to attract the attention of physicists and mathematicians in the most diverse settings, such as Rademacher matrices [69], supercritical sparse Wigner matrices [70], spiked Gaussian random matrices [71], sums or products of invariant random matrices [72], sparse networks with Gaussian weights [73], Wigner matrices without Gaussian tails [74], rank-one deformation of Gaussian ensembles [75], random deformations of matrices [76], generalized sample covariance matrices [77] (and references therein), as well as many others.

B. Appendix: Edelman-Persson algorithm for fast histogramming of scaled largest eigenvalue of huge Gaussian matrices [31]

The *Gaussian Unitary Ensemble* (GUE) is defined as the set of Hermitian $N \times N$ matrices H, where the diagonal elements H_{jj} and the upper triangular elements $H_{jk} = u_{jk} + \mathrm{i}v_{jk}$ are independent Gaussians with zero-mean, and

$$\begin{cases} \mathrm{Var}(H_{jj}) = 1, & 1 \le j \le N, \\ \mathrm{Var}(u_{jk}) = \mathrm{Var}(v_{jk}) = \frac{1}{2}, & 1 \le j < k \le N. \end{cases} \tag{67}$$

Since a sum of Gaussians is a new Gaussian, an instance of these matrices can be created conveniently in MATLAB[5]

```
H = randn(N)+i*randn(N);
H = (H+H')/2;
```

The largest eigenvalue $\tilde{r}_1$ of this matrix is about $2\sqrt{N}$. To get a distribution that converges as $N \to \infty$, the shifted and scaled largest eigenvalue $\chi_{\beta=2}$ is calculated as (see Eq. (30))

$$\chi_{\beta=2} = N^{\frac{1}{6}} \left(\tilde{r}_1 - 2\sqrt{N} \right). \tag{68}$$

It is now in principle straightforward to compute the distribution for $\chi_{\beta=2}$ by simulation

```
for ii = 1:trials
  H = randn(N)+i*randn(N);
  H = (H+H')/2;
  r1 = max(eig(H));
  chibeta = N^(1/6)*(r1-2*sqrt(N));
  % Store chibeta
  % Create and plot histogram
end
```

The problem with this technique is that the computational requirements and the memory requirements grow fast with N, which should be as large as possible in order to be a good approximation of infinity. Just storing the matrix H requires N^2 double-precision numbers. Furthermore, computing all the eigenvalues of a full Hermitian matrix requires a computing time proportional to N^3. This means that it will take many days to create a smooth histogram by simulation, even for relatively small values of N.

To improve upon this situation, another matrix can be studied that has the same eigenvalue distribution as H above. In [78], it was shown that this is true for the following *symmetric* matrix when $\beta = 2$:

$$H_\beta \sim \frac{1}{\sqrt{2}} \begin{pmatrix} \mathcal{N}(0,2) & \chi_{(n-1)\beta} & & & \\ \chi_{(n-1)\beta} & \mathcal{N}(0,2) & \chi_{(n-2)\beta} & & \\ & \ddots & \ddots & \ddots & \\ & & \chi_{2\beta} & \mathcal{N}(0,2) & \chi_\beta \\ & & & \chi_\beta & \mathcal{N}(0,2) \end{pmatrix}. \tag{69}$$

---

[5] This code generates eigenvalues distributed according to $\mathcal{P}(x_1, \dots, x_N) = \exp[-(1/2)\sum_k x_k^2 - \sum_{i \ne j} \log|x_i - x_j|]$. In order to match the joint probability density as given in (18), we need to rescale the eigenvalues by $\sqrt{2\beta N} = 2\sqrt{N}$.

Here, $\mathcal{N}(0,2)$ is a zero-mean Gaussian with variance 2, and χ_d is the square-root of a χ^2 distributed number with d degrees of freedom. Note that the matrix is symmetric, so the subdiagonal and the superdiagonal are always equal.

This matrix has a tridiagonal sparsity structure, and only $2N$ double-precision numbers are required to store an instance of it. The time for computing the largest eigenvalue is proportional to N, either using Krylov subspace based methods or the method of bisection [79].

In MATLAB, the built-in function `eigs` can be used, although that requires dealing with the sparse matrix structure. There is also a large amount of overhead in this function, which results in a relatively poor performance. It is based on the method of bisection, and requires just two ordinary MATLAB vectors as input, corresponding to the diagonal and the subdiagonal.

It also turns out that only the first $10N^{\frac{1}{3}}$ components of the eigenvector corresponding to the largest eigenvalue are significantly greater than zero. Therefore, the upper-left N_{cutoff} by N_{cutoff} submatrix has the same largest eigenvalue (or at least very close), where

$$N_{\text{cutoff}} \approx 10N^{\frac{1}{3}}. \tag{70}$$

Matrices of size $N = 10^{12}$ can then easily be used since the computations can be done on a matrix of size only $10N^{\frac{1}{3}} = 10^5$. Also, for these large values of N the approximation $\chi_N^2 \approx N$ is accurate.

A histogram of the distribution for $N = 10^9$ can now be created using the code below.

```
N=1e9;
nrep=1e4;
beta=2;

cutoff=round(10*N^(1/3));
d1=sqrt(N-1:-1:N+1-cutoff)'/2/sqrt(N);

ls=zeros(1,nrep);
for ii=1:nrep
  d0=randn(cutoff,1)/sqrt(N*beta);
  ls(ii)=maxeig(d0,d1);
end

ls=(ls-1)*N^(2/3)*2;

histdistr(ls,-7:0.2:3)
```

where the function `histdistr` below is used to histogram the data. It assumes that the histogram boxes are equidistant.

```
function [xmid,H]=histdistr(ls,x)

dx=x(2)-x(1);
H=histc(ls,x);
H=H(1:end-1);
H=H/sum(H)/dx;
xmid=(x(1:end-1)+x(2:end))/2;

bar(xmid,H)
grid on
```

The resulting distribution is shown in Figure 4, together with distributions for $\beta = 1$ and $\beta = 4$. The plots also contain solid curves representing the "true solutions" (see [31] for a Matlab code to produce the theoretical Tracy-Widom distributions (32) and densities by solving numerically the associated Painlevé equations).

C. Appendix: brief comments on the non-hermitian case (log-case in the plane)

For non-hermitian matrices (e.g. from the complex Ginibre ensemble), the behavior of the eigenvalue with largest modulus $r_2 = \max_j |z_j|$ is similar to what happens for r_1 in the real case, with some important differences. The same three regimes as in the real case (see Eq. (37)) exist, plus a fourth regime of intermediate fluctuations [80].

For typical fluctuations of the complex Ginibre ensemble (defined by the joint probability density in Eq. (16)), Rider [81] has proved the following remarkable limiting result for the typical fluctuations of r_2. Let $\gamma_N = \log N - 2\log\log N - \log 2\pi$, $a_N = \sqrt{4N\gamma_N}$ and $b_N = 1 + \sqrt{\gamma_N/(4N)}$. Then, the rescaled variable $a_N(r_2 - b_N)$ converges in distribution as $N \to \infty$ to a standard Gumbel variable, i.e. setting $Q_N(w) = \text{Prob}[r_2 \le w]$ we have

$$\lim_{N\to\infty} Q_N\left(b_N + \frac{w}{a_N}\right) = G(w) = \mathrm{e}^{-\mathrm{e}^{-w}} \ . \tag{71}$$

An interesting corollary of the centering constant b_N being larger than 1 is that the eigenvalue with largest modulus tends (with large probability) to lie *outside* the unit disc as $N \to \infty$. It is interesting to contrast this with the known cases for real Gaussian spectra: the limit Tracy-Widom distributions (32) of the maximal eigenvalue (after subtracting off the edge and scaling by an increasing factor) all have *negative* mean.

A similar result has been recently established [83] for a general class of radially symmetric external potentials $V(z) = V(|z|)$. In contrast with the Tracy-Widom law governing the typical fluctuations of the similar observable r_1 in the real-spectrum case, the Gumbel law arises naturally in the Extreme Value statistics of *independent* (and identically distributed) random variables (see [84] for a pedagogical account). The appearance of a "simple" Gumbel law in a problem of strongly correlated random variables is superficially quite surprising: however, Kostlan in [85] had managed to integrate out the angular variables θ_j of the eigenvalues $z_j = |z_j|\mathrm{e}^{\mathrm{i}\theta_j}$ of a complex Ginibre matrix, and showed that, up to a random reshuffling, the eigenvalues moduli $|z_i|$ are indeed distributed as a collection of *independent* (although not identically distributed) χ random variables: $(|z_1|, \ldots, |z_N|) \overset{d}{=} \sigma(\xi_1/\sqrt{N}, \ldots, \xi_N/\sqrt{N})$ where $\xi_1, \ldots, \xi_N$ are independent positive random variables with density [6]

$$x \mapsto \frac{2}{\Gamma(k)} x^{2k-1}\mathrm{e}^{-x^2}, \qquad k = 1, \ldots, N \ , \tag{72}$$

and σ is a random permutation uniformly distributed in S_N (Reproducing Kostlan's result is left as an exercise - happy to provide guidance).

For works on large deviations of the spectral radius (towards the bulk, and outside the bulk), I refer to [80, 82, 86–89]. Borrowing almost verbatim from [80]: While the Gumbel law describes the probability of typical fluctuations of r_2, its atypically large fluctuations are described by large deviation tails [82], much like the Gaussian case in Eq. (37). To summarize

$$Q_N(w) \sim \begin{cases} \mathrm{e}^{-N^2\Phi_-(w)+o(N^2)} \ , \text{ for } 0 < (1-w) = \mathcal{O}(1) \\ \\ G(a_N(w-b_N)) \ , \text{ for } (w-b_N) = \mathcal{O}(a_N^{-1}) \\ \\ 1 - \mathrm{e}^{-N\Phi_+(w)+o(N)} \ , \text{ for } 0 < (w-b_N) = \mathcal{O}(1) \ , \end{cases} \tag{73}$$

where[7] $\Phi_+(w)$ and $\Phi_-(w)$ can be explicitly computed [82]

$$\Phi_-(w) = \frac{1}{4}(4w^2 - w^4 - 4\ln w - 3) \ , \text{ for } \ 0 < w < 1 \ , \tag{74}$$

$$\Phi_+(w) = w^2 - 2\ln w - 1 \ , \ \text{ for } \ w > 1 \ . \tag{75}$$

It is not hard to check that the right tail of the central scaling function $G(a_N(w - b_N))$ for $w - b_N \gg 1/a_N$ matches smoothly with the right large deviation tail (I refer to [80] for details and leave this check as an exercise).

What about the left tail? As in the case of the right tail above, and consistently with what happens in the Gaussian case as well, one would naïvely expect a similar matching on the left tail also. However, this does not happen [82]! To see this, consider the left asymptotic tail of the central Gumbel distribution. Using $G(z) \sim \mathrm{e}^{-\mathrm{e}^{-z}}$ as $z \to -\infty$, the PDF $Q'_N(w)$ has a super-exponential tail for large negative argument. In contrast, as $w \to 1$ from the left, using $\Phi_-(w) \sim (4/3)(R_\star - w)^3$ (with $R_\star = 1$ for the complex Ginibre case) one sees from the first line of Eq. (73) that $Q'_N(w) \sim \mathrm{e}^{-(4/3)\,N^2(R_\star - w)^3}$. Clearly, this can not match with the super exponential tail of the central Gumbel regime. This represents a puzzle, since, in most of the known cases, in particular for rotationally invariant matrix models, there is a smooth matching between the central part and the large deviation tails [28].

---

[6] In other words $\xi_k^2 \overset{d}{=} \chi^2_{2k}/2$.

[7] For simplicity, I keep the same notation $\Phi_\pm(w)$ as in the real Gaussian case, even though the form of the functions is clearly different in the two cases.

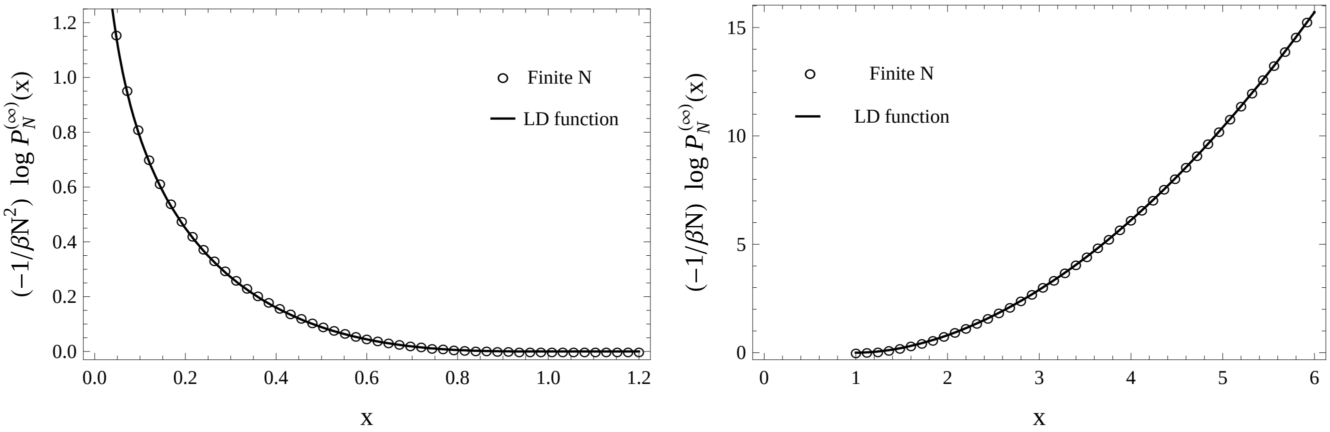

FIG. 7. Comparison between the large deviation functions $\Phi_-(x)$ (left panel) in (74) and $\Phi_+(x)$ (right panel) in (75) with an available finite-N formula (dots) for $\beta = 2$ with $N = 250$. Figure taken from [82].

In fact, this mismatch in the left tail is not only restricted to Ginibre matrices, i.e. for a quadratic potential $V(z) = |z|^2/2$, but also holds for a much wider class of sufficiently confining (and spherically symmetric) potentials, e.g. $V(z) \sim |z|^p$ with $p > 1$. For such spherically symmetric potentials, the Cumulative Distribution Function of r_2, denoted by $Q_N(w)$, has again a central part described by a Gumbel law [90, 91]. In addition, the left large deviation $\Phi_-(w)$ also exhibits a cubic behavior as $w \to R_\star$ from below [92]. Thus the problem of mismatch at the left tail also exists for generic spherically symmetric potentials.

In the paper [80], the authors solved this interesting puzzle by showing that there exists a novel intermediate deviation regime for $(R_\star - w) \sim \Delta_N = \mathcal{O}(1/\sqrt{N})$, which interpolates smoothly between the left large deviation tails for $0 < (R_\star - w) = \mathcal{O}(1)$ and the central part, given by the Gumbel law, for $(b_N - w) = \mathcal{O}(1/\sqrt{N}\ \ln N)$ [see Eq. (73)]. In this intermediate regime, the Cumulative Distribution function $Q_N(w)$ takes the scaling form

$$Q_N(w) \sim \exp\left[-\tfrac{R_\star}{\Delta_N}\phi_I\left(\tfrac{w-R_\star}{\Delta_N}\right)\right] \ , \tag{76}$$

where $R_\star$ is again the soft edge of the equilibrium density in the plane, and $\Delta_N \sim \mathcal{O}(1/\sqrt{N})$ has an explicit expression in term of N, $R_\star$ and the equilibrium density in the bulk [80].

The intermediate rate function $\phi_I(y)$ is universal, i.e., independent of the details of the confining potential $V(z)$, and is given by the exact formula

$$\phi_I(y) = -\int_0^\infty \mathrm{d}v \log\left(\frac{1}{2}\mathrm{erfc}(-y-v)\right) \ , \tag{77}$$

in terms of the complementary error function. The asymptotic behaviors of this rate function $\phi_I(y)$ are

$$\phi_I(y) \sim \begin{cases} \dfrac{|y|^3}{3} + |y|\ln|y| + \mathcal{O}(y) \ , \quad y \to -\infty \\ \\ \dfrac{\mathrm{e}^{-y^2}}{4\sqrt{\pi}y^2} \ , \quad y \to +\infty \ . \end{cases} \tag{78}$$

Note that this scaling function $\phi_I(y)$ appeared in previous works, in intermediate computations, on Ginibre matrices [20] section 15.5.2 (see also Ref. [91]) but without the interpretation as intermediate deviation function interpolating between the left large deviations and the typical fluctuations of r_2.

To summarize, there are now *four* regimes for the full Cumulative Distribution Function $Q_N(w)$ of the complex

Ginibre ensemble, including the new intermediate deviation regime discovered in [80]

$$Q_N(w) \sim \begin{cases} \mathrm{e}^{-N^2\Phi_-(w)} \ , \ \text{for } 0 < (R_\star - w) = \mathcal{O}(1) \\ \\ \mathrm{e}^{-\frac{R_\star}{\Delta_N}\phi_I\left(\frac{w-R_\star}{\Delta_N}\right)} \ , \ \text{for } (R_\star - w) = \mathcal{O}(\Delta_N) \\ \\ G(a_N(w-b_N)) \ , \ \text{for } (w-b_N) = \mathcal{O}(a_N^{-1}) \\ \\ 1 - \mathrm{e}^{-N\Phi_+(w)} \ , \ \text{for } 0 < (w-b_N) = \mathcal{O}(1) \ . \end{cases} \tag{79}$$

The presence of this intermediate new regime now ensures a smooth matching between all four regimes (see again [80] for details).

V. LECTURE 2/3 - REPLICA DERIVATION OF RIGHT LARGE DEVIATION TAIL FOR THE GAUSSIAN ORTHOGONAL ENSEMBLE ($\beta = 1$)

In this section, I will show how to re-obtain the formula (41) for the right large deviation function using a completely different method based on the physics of disordered systems. The derivation is valid for the Gaussian Orthogonal Ensemble $\beta = 1$ (although it could be easily extended to $\beta = 2$) and is contained as a special case of a more general theory developed by Fyodorov and Le Doussal [29].

Consider the standard GOE ensemble (Gaussian Orthogonal Ensemble) of real symmetric random matrices, characterized by the joint distribution of matrix entries in the upper triangle

$$\mathcal{P}(H_{11}, \ldots, H_{NN}) = \prod_{i=1}^{N} \frac{\mathrm{e}^{-\frac{N}{2}H_{ii}^2}}{\sqrt{2\pi(1/N)}} \prod_{i<j} \frac{\mathrm{e}^{-NH_{ij}^2}}{\sqrt{2\pi(1/2N)}} \tag{80}$$

and by $\mathcal{O}(1)$ real eigenvalues distributed according to

$$\mathcal{P}_{\beta=1,N}(x_1, \ldots, x_N) = \frac{1}{\mathcal{Z}_{\beta=1,N}} \mathrm{e}^{-\beta E(x_1,\ldots,x_N)} \ , \tag{81}$$

$$E(x_1, \ldots, x_N) = -\frac{1}{2}\sum_{i\neq j} \log|x_i - x_j| + N\sum_k \frac{x_k^2}{2} \ . \tag{82}$$

We are again interested in the distribution of the largest eigenvalue

$$r_1 = \max_j x_j \approx \mathcal{O}(1) \text{ for large } N \ . \tag{83}$$

Using the Courant-Fisher definition of eigenvector, we may write

$$r_1 = \max_{\boldsymbol{v}} \frac{(\boldsymbol{v}, H\boldsymbol{v})}{|\boldsymbol{v}|^2} \ , \tag{84}$$

where $(\boldsymbol{v}, H\boldsymbol{v}) = \boldsymbol{v}^T H \boldsymbol{v}$ is the dot product in the space of N-dimensional real vectors $\boldsymbol{v}$, which we will further normalize as $|\boldsymbol{v}|^2 = \sum_k v_k^2 = N$.

Given the definition of r_1 as the maximum of a quantity, we can set up a statistical mechanics framework to represent this maximum in a more convenient form. Consider the canonical distribution of N-dimensional real vectors at inverse temperature $\tilde{\beta}$

$$P_{\tilde{\beta}}(\boldsymbol{v}) = \frac{1}{Z_N^{(H)}(\tilde{\beta})} \mathrm{e}^{\frac{\tilde{\beta}}{2}(\boldsymbol{v},H\boldsymbol{v})} \delta(|\boldsymbol{v}|^2 - N) \ , \tag{85}$$

whose partition function is

$$Z_N^{(H)}(\tilde{\beta}) = \int \mathrm{d}\boldsymbol{v} \ \mathrm{e}^{\frac{\tilde{\beta}}{2}(\boldsymbol{v},H\boldsymbol{v})} \delta(|\boldsymbol{v}|^2 - N) \ . \tag{86}$$

Using the Laplace method to evaluate the integral for large $\tilde{\beta}$ (see Appendix V A for details), we can write from (84)

$$Z_N^{(H)}(\tilde{\beta}) \approx \mathrm{e}^{\frac{\tilde{\beta}}{2}\overbrace{\max_{|\boldsymbol{v}|^2=N}(\boldsymbol{v},H\boldsymbol{v})}^{Nr_1}}\ , \tag{87}$$

from which it follows that

$$\boxed{r_1 = \lim_{\tilde{\beta}\to\infty} \frac{2}{\tilde{\beta}N} \log Z_N^{(H)}(\tilde{\beta})}\ . \tag{88}$$

Note that r_1 is a random variable, which depends on the realization of the "disorder" in the random matrix H. Suppose we now wanted to compute the average $\langle r_1\rangle_H \sim \mathcal{O}(1)$ over the ensemble of random matrices H for large N (which according to our normalization would be equal to $\sqrt{2}$). We would therefore need to compute the following average of the *logarithm* of the partition function integral

$$\langle \log Z_N^{(H)}(\tilde{\beta})\rangle_H = \int \mathrm{d}H_{11}\cdots \mathrm{d}H_{NN}\mathcal{P}(H_{11},\ldots,H_{NN}) \log \int \mathrm{d}\boldsymbol{v}\ \mathrm{e}^{\frac{\tilde{\beta}}{2}(\boldsymbol{v},H\boldsymbol{v})}\delta(|\boldsymbol{v}|^2-N)\ . \tag{89}$$

What is the problem here? Eq. (89) defines a so called *quenched*[8] average: there are two nested sources of randomness, (i) the disorder in the matrix H, and (ii) the Gibbs-Boltzmann distribution of the auxiliary degrees of freedom $\boldsymbol{v}$ at inverse temperature $\tilde{\beta}$. A single instance of H is selected and kept fixed, while the $\boldsymbol{v}$ degrees of freedom equilibrate at inverse temperature $\tilde{\beta}$, before another instance of the H disorder is picked, and the process is repeated. In thermodynamical terms, a quenched average rests on the separation between two temporal scales, the "fast" equilibration of the $\boldsymbol{v}$ degrees of freedom at fixed temperature and at fixed instance of the disorder, and a "slower" scale of change of the background disorder. This should be contrasted with the *annealed*[9] scheme, which is only approximate but way easier to handle analytically, consisting in treating the averages over the disorder and over the Gibbs-Boltzmann distribution on the same footing, and simultaneously. We will not consider annealed calculations here – for more information, see [93, 94].

Clearly, the only obvious way to crack the integral (89) is to solve the $\boldsymbol{v}$-integral *first*, take the logarithm of the result, and take the H-integrals *last*. Unfortunately, this procedure fails in most cases, because the $\boldsymbol{v}$-integral cannot in general be solved exactly for a fixed instance of H (or – for different models – of the so called *disorder*, namely the randomness inherent to the parameters entering the definition of the "cost function" that multiplies $\tilde{\beta}$ in the exponent of the Gibbs-Boltzmann distribution).

It would therefore be very helpful to make some headway if we were able somehow to take the average over the disorder H *first*, and the $\boldsymbol{v}$-integral *last* – in the hope that swapping the order of integration would make the integrals more friendly to tackle.

A heuristic recipe to do just that originated in the "theory of spin glasses" [93] in the 70s. Doing this swapping of integrals in a fully rigorously manner is quite challenging even in the simplest possible instances, though considerable progress has been achieved in the last decades in evaluating such averages in a mathematically controllable way in the case when the cost function is normally distributed, see e.g. [95–97]. Even when the cost function is not normally distributed, progress is still possible within the powerful but heuristic method of Theoretical Physics, known as the "replica trick", see e.g. [98].

The main idea rests on the exact identity

$$\langle \log z\rangle = \lim_{n\to 0}\frac{1}{n}\log\langle z^n\rangle\ , \tag{90}$$

which can be proven by noting that $\langle z^n\rangle = \langle 1+n\log z+o(n)\rangle = \langle 1\rangle + n\langle\log z\rangle + \ldots = 1+n\langle \log z\rangle+\ldots$, where we used linearity of expectations, and normalization $\langle 1\rangle = 1$.

While the identity (90) is mathematically fully rigorous, and requires n to be real and in the vicinity of zero, the way it is implemented in replica calculations is as follows: assume first that n is an integer.

---

[8] From Merriam-Webster dictionary. *Quench* [transitive verb]: to cool (something, such as heated metal) suddenly by immersion (as in oil or water).

[9] *Anneal* [transitive verb]: to heat and then cool slowly (a material, such as steel or glass) usually for softening and making less brittle.

This approach assumes that the mean value we are after can be found not from directly calculating the average, but by considering the expectation of the integer moments of the partition function, frequently called in the physical literature the "replicated" disorder averaged partition function

$$\left\langle\left[Z_N^{(H)}(\tilde{\beta})\right]^n\right\rangle_H \tag{91}$$

and subsequently taking the limit[10] $n \rightsquigarrow 0$ to recover the averaged log

$$\langle\log Z_N^{(H)}(\tilde{\beta})\rangle_H = \lim_{n\rightsquigarrow 0}\frac{1}{n}\log\left\langle\left[Z_N^{(H)}(\tilde{\beta})\right]^n\right\rangle_H . \tag{92}$$

Note that in this way the annoying logarithm has been effectively neutralized and forced out of the average. Moreover, the integer nature of n (at least initially) allows to replicate the $\boldsymbol{v}$ integral n-times, which simply results in a "larger" integral that allows us to swap the integration order and perform the average over the disorder first (see below).

Eventually, one could compute the large-N limit of the average position of the largest eigenvalue by the following chain of limits[11]

$$\langle r_1\rangle = \lim_{N\to\infty}\frac{1}{N}\lim_{\tilde{\beta}\to\infty}\frac{2}{\tilde{\beta}}\lim_{n\rightsquigarrow 0}\frac{1}{n}\log\left\langle\left[Z_N^{(H)}(\tilde{\beta})\right]^n\right\rangle_H . \tag{93}$$

I leave the calculation of the average largest eigenvalue following (93) as an exercise, which should be doable relatively easily after we engage in the a priori more complicated task of computing the *full distribution* (and not just the average) of r_1 (in the large deviation sense). It turns out that the replica formalism described above can indeed be slightly modified to give access to more general observables.

Consider indeed again the replicated average

$$\left\langle\left[Z_N^{(H)}(\tilde{\beta})\right]^n\right\rangle_H , \tag{94}$$

where the average is taken over the joint distribution (80). We can write

$$\left\langle\left[Z_N^{(H)}(\tilde{\beta})\right]^n\right\rangle_H = \left\langle e^{n\log Z_N^{(H)}(\tilde{\beta})}\right\rangle_H \tag{95}$$

and setting $n = -s/\tilde{\beta}$ (with $s<0$), we can write

$$\lim_{\tilde{\beta}\to\infty}\left\langle e^{\frac{-s}{\tilde{\beta}}\log Z_N^{(H)}(\beta)}\right\rangle_H = \left\langle e^{-s\frac{N}{2}r_1}\right\rangle_H , \tag{96}$$

where we have used Eq. (88).

Therefore, the moment generating function of the largest GOE eigenvalue (at *finite* N) – encoding information about its *full distribution* – can be in principle retrieved from the following non-standard double-scaling limit[12]

$$\left\langle e^{-s\frac{N}{2}r_1}\right\rangle_H = \lim_{\tilde{\beta}\to\infty}\left\langle\left[Z_N^{(H)}(\tilde{\beta})\right]^{-s/\tilde{\beta}}\right\rangle_H , \tag{97}$$

where the replica index n and the fictitious temperature $\tilde{\beta}$ are coupled in a non-trivial way. I now proceed to compute the r.h.s. of (97).

We have for integer n (ignoring pre-factors from now on)

$$\begin{aligned}\left\langle\left[Z_N^{(H)}(\tilde{\beta})\right]^n\right\rangle_H &\propto \int\prod_{a=1}^n d\boldsymbol{v}_a\prod_{a=1}^n\delta(|\boldsymbol{v}_a|^2-N)\int\prod_{i=1}^N dH_{ii}e^{-\frac{N}{2}\sum_{i=1}^N H_{ii}^2}\times\\ &\times\prod_{i<j}dH_{ij}e^{-N\sum_{i<j}^N H_{ij}^2}e^{\frac{\tilde{\beta}}{2}\sum_{a=1}^n\sum_{i,j}v_{ia}H_{ij}v_{ja}}\\ &=\int\prod_{a=1}^n d\boldsymbol{v}_a\prod_{a=1}^n\delta(|\boldsymbol{v}_a|^2-N)\exp\left[\frac{\tilde{\beta}^2}{8N}\sum_{i,j}\left(\sum_a v_{ia}v_{ja}\right)^2\right] ,\end{aligned} \tag{98}$$

---

[10] I use the wiggly arrow $\rightsquigarrow$ to denote the "replica limit" procedure as follows: first convert $n\in\mathbb{R}$ to an integer. Then evaluate the corresponding observable as an explicit function of the integer n. Then pretend that n could be analytically continued in the vicinity of zero without ambiguities.

[11] In practice, though, a second mathematically questionable step is needed, namely the exchange of the order of limits, with the $N\to\infty$ limit taken *first* (see below).

[12] Of course, the initial step of having to promote n to an integer is still necessary to kick the logarithm out of the way and perform the disorder average first.

where we used the Gaussian integral

$$\int_{-\infty}^{\infty} \mathrm{d}x\ \mathrm{e}^{-ax^2+bx} \propto \mathrm{e}^{\frac{b^2}{4a}} \tag{99}$$

and we have replicated the partition function integral (86) n times. Indeed, each of the diagonal integral would read

$$\int \mathrm{d}H_{ii} \mathrm{e}^{-\frac{N}{2}H_{ii}^2+\frac{\tilde{\beta}}{2}\sum_a v_{ia}^2 H_{ii}} \propto \mathrm{e}^{\frac{1}{2N}\left[\frac{\tilde{\beta}}{2}\sum_a v_{ia}^2\right]^2} = \mathrm{e}^{\frac{\tilde{\beta}}{8N}\left(\sum_a v_{ia}^2\right)^2}\ , \tag{100}$$

while the off-diagonal integral reads

$$\int \mathrm{d}H_{ij} \mathrm{e}^{-NH_{ij}^2+\tilde{\beta}\sum_a v_{ia}v_{ja}H_{ij}} \propto \mathrm{e}^{\frac{1}{4N}\left(\tilde{\beta}\sum_a v_{ia}v_{ja}\right)^2}\ . \tag{101}$$

Therefore, overall we have

$$\int \prod_i \mathrm{d}H_{ii} \prod_{i<j} \mathrm{d}H_{ij}\,(\dots) \propto \mathrm{e}^{\frac{\tilde{\beta}^2}{8N}\sum_{i,j}\left(\sum_a v_{ia}v_{ja}\right)^2}\ . \tag{102}$$

We now note that

$$\frac{\tilde{\beta}^2}{8N}\sum_{i,j}\left(\sum_a v_{ia}v_{ja}\right)^2 = \frac{\tilde{\beta}^2}{8N}\sum_{a,b}\left(\sum_i v_{ia}v_{ib}\right)\left(\sum_j v_{ja}v_{jb}\right) = \frac{\tilde{\beta}^2}{8N}\sum_{a,b}\left(\sum_i v_{ia}v_{ib}\right)^2\ . \tag{103}$$

We now introduce in a standard way the $n \times n$ overlap matrix Q with elements

$$Q_{ab} = \frac{1}{N}\boldsymbol{v}_a^T\boldsymbol{v}_b = \frac{1}{N}\sum_i v_{ia}v_{ib}\ , \tag{104}$$

where $\boldsymbol{v}_a = (v_{1a},\dots,v_{Na})^T$ is a N dimensional column vector (and we have n of them). The overlap matrix Q has the following properties:

- it is symmetric
- $Q_{aa} = 1$ for all a
- it is positive semi-definite[13]

Enforcing the definition of the overlap matrix with a delta, we can write:

$$\left\langle\left[Z_N^{(H)}(\tilde{\beta})\right]^n\right\rangle_H \propto \int\prod_{a,b}\mathrm{d}Q_{ab}\exp\left[\frac{N\tilde{\beta}^2}{8}\sum_{a,b}Q_{ab}^2\right]\int\prod_{a=1}^n \mathrm{d}\boldsymbol{v}_a\prod_{a=1}^n\delta(|\boldsymbol{v}_a|^2-N)\prod_{a,b}\delta\left(NQ_{ab}-\sum_i v_{ia}v_{ib}\right)\ . \tag{105}$$

Moreover

$$\delta(|\boldsymbol{v}_a|^2-N) = \delta\left(\sum_i v_{ia}^2 - N\right) = \delta(NQ_{aa}-N) \propto \delta(Q_{aa}-1)\ , \tag{106}$$

therefore

$$\left\langle\left[Z_N^{(H)}(\tilde{\beta})\right]^n\right\rangle_H \propto \int\prod_{a,b}\mathrm{d}Q_{ab}\exp\left[\frac{N\tilde{\beta}^2}{8}\sum_{a,b}Q_{ab}^2\right]\prod_{a=1}^n\delta(Q_{aa}-1)\underbrace{\int\prod_{a=1}^n \mathrm{d}\boldsymbol{v}_a\prod_{a,b}\delta\left(NQ_{ab}-\sum_i v_{ia}v_{ib}\right)}_{\Phi_{N,n}(Q)}\ . \tag{107}$$

---

[13] This means that $\boldsymbol{x}^TQ\boldsymbol{x} \geq 0$ if $\boldsymbol{x} \neq 0$. We can show this as follows: $\sum_{a,b}x_aQ_{ab}x_b = \frac{1}{N}\sum_{a,b}\sum_i x_av_{ai}v_{bi}x_b = \frac{1}{N}\sum_i\left(\sum_a x_av_{ba}\right)\left(\sum_b x_bv_{bi}\right) = \frac{1}{N}\sum_i\left(\sum_a x_av_{ai}\right)^2 \geq 0$.

Let us now compute the entropic term $\Phi_{N,n}(Q)$ as follows

$$\begin{aligned}\Phi_{N,n}(Q) &= \int \prod_{a=1}^{n} \mathrm{d}\boldsymbol{v}_a \prod_{a,b} \delta\left(NQ_{ab} - \sum_i v_{ia} v_{ib} \right) \\ &\propto \int \prod_{a,b} \mathrm{d}\hat{Q}_{a,b} \mathrm{e}^{\mathrm{i}N \sum_{a,b} \hat{Q}_{ab} Q_{a,b}} \left[\int \prod_{a=1}^{n} \mathrm{d}v_a \mathrm{e}^{-\mathrm{i} \sum_{a,b} v_a \hat{Q}_{ab} v_b} \right]^N ,\end{aligned} \tag{108}$$

where we used the Fourier representation of the delta function

$$\delta(x) = \int_{-\infty}^{\infty} \frac{\mathrm{d}k}{2\pi} \mathrm{e}^{\mathrm{i}kx} . \tag{109}$$

The multiple v_a integral is Gaussian[14] and therefore results in (omitting constants)

$$\Phi_{N,n}(Q) \propto \int \prod_{a,b} \mathrm{d}\hat{Q}_{ab} \mathrm{e}^{\mathrm{i}N \sum_{a,b} \hat{Q}_{ab} Q_{a,b}} (\det \hat{Q})^{-N/2} \propto (\det Q)^{(N-n-1)/2} . \tag{110}$$

The result follows noticing that the integral is quite close to the Ingham-Siegel integral formula [15][99, 100]

$$J_{N,p}^{IS}(Q) = \int_{\hat{Q}>0} \mathrm{d}\hat{Q} \ \mathrm{e}^{\mathrm{Tr}\hat{Q}Q} (\det \hat{Q})^p = \pi^{n(n-1)/4} \prod_{k=1}^{n} \Gamma\left(p + \frac{k+1}{2} \right) \det Q^{-\left(p+\frac{n+1}{2}\right)} \tag{111}$$

valid for $p > 0$ and positive definite real symmetric matrices $\hat{Q}$ and Q of size n. This integral was generalized by Fyodorov [101] by (i) lifting the requirement that the integration matrix $\hat{Q}$ be positive definite, and (ii) allowing $p < 0$, which is needed in our case. The final result is (omitting pre-factors) as given in (110) and valid for $N \geq n + 1$.

The leading large-N term therefore is

$$\boxed{\Phi_{N,n}(Q) \approx (\det Q)^{\frac{N}{2}}} . \tag{112}$$

Alternatively, one could have proceeded immediately from (108) with a saddle-point evaluation for large N writing

$$\Phi_{N,n}(Q) \propto \int \prod_{a,b} \mathrm{d}\hat{Q}_{ab} \ \mathrm{e}^{NS[\hat{Q},Q]} , \tag{113}$$

with

$$\begin{aligned}S[\hat{Q}, Q] &= \mathrm{i} \sum_{a,b} \hat{Q}_{ab} Q_{ab} + \log \int \prod_{a=1}^{n} \mathrm{d}v_a \mathrm{e}^{-\mathrm{i} \sum_{a,b} v_a \hat{Q}_{ab} v_b} & (114) \\ &= \mathrm{i} \sum_{a,b} Q_{ab} \hat{Q}_{ab} - \frac{1}{2} \log \det(\hat{Q}) + \dots , & (115)\end{aligned}$$

where we neglect irrelevant constants in the $n \to 0$ limit.

Evaluating the stationary point of this action yields

$$\frac{\partial S}{\partial \hat{Q}_{ab}} = 0 \Rightarrow \mathrm{i}Q_{ab} - \mathrm{i} \frac{\int \prod_{r=1}^{n} \mathrm{d}v_r \ v_a v_b e^{-\mathrm{i} \sum_{a,b} v_a \hat{Q}_{ab} v_b}}{\int \prod_{r=1}^{n} \mathrm{d}v_r e^{-\mathrm{i} \sum_{a,b} v_a \hat{Q}_{ab} v_b}} = 0 \Rightarrow Q_{ab} = [\hat{Q}^{-1}]_{ba} , \tag{116}$$

where we have used the log-det identity given in Appendix V B.

---

[14] $\int_{\mathbb{R}^n} \mathrm{d}^n \vec{v} \ \mathrm{e}^{-\frac{1}{2} \vec{v}^T M \vec{v}} = \sqrt{\frac{(2\pi)^n}{\det M}}$.

[15] It is a matrix generalization of the Gamma integral $\int_{f>0} \mathrm{d}f f^p \mathrm{e}^{-fq} = \Gamma(p+1) q^{-(p+1)}$.

Inserting the saddle-point $\hat{Q} = Q^{-1}$ solution back into the action (115) yields

$$S[\hat{Q}, Q] = \mathrm{i} \sum_{a,b} Q_{ab}[Q^{-1}]_{ba} - \frac{1}{2} \log\det Q^{-1} + \ldots = \mathrm{i} \sum_{a} (QQ^{-1})_{aa} + \frac{1}{2} \log\det Q = \mathrm{i}n + \frac{1}{2} \log\det Q \ . \tag{117}$$

In the $n \to 0$ limit, the leading term of $\Phi_{N,n}(Q)$ therefore comes out as expected from the Ingham-Siegel exact evaluation (see Eq. (110)), namely

$$\Phi_{N,n}(Q) \propto \exp\left[\frac{N}{2} \log\det Q\right] \ . \tag{118}$$

Inserting this back into Eq. (107), we can write

$$\left\langle \left[Z_N^{(H)}(\tilde{\beta})\right]^n \right\rangle_H \propto \int \prod_{a,b} \mathrm{d}Q_{ab} \exp\left[\frac{N\tilde{\beta}^2}{8} \sum_{a,b} Q_{ab}^2\right] \prod_{a=1}^{n} \delta(Q_{aa} - 1)(\det Q)^{(N-n-1)/2} = \int \mathrm{d}Q \ (\det Q)^{(-n-1)/2} \mathrm{e}^{NS[Q]} \ , \tag{119}$$

where the integration runs over positive semi-definite matrices Q of size n, with diagonal elements equal to one, and the action $S[Q]$ is given by

$$S[Q] = \frac{\tilde{\beta}^2}{8} \mathrm{Tr} Q^2 + \frac{1}{2} \log\det Q \ . \tag{120}$$

This is equivalent to Eq. (25) of the Fyodorov-Le Doussal paper [29].

A few observations are in order:

1. The replica approach as developed in this section leads to an action of the form $\sim NS[Q]$ (so of order $\mathcal{O}(N)$), but is seemingly unable to capture either (i) the typical order $\mathcal{O}(N^{-2/3})$ of fluctuations of r_1 around its mean, or (ii) the atypical fluctuations to the *left* of the mean, which are of order $\sim \mathcal{O}(N^2)$. How to recover the law of typical fluctuations (Tracy-Widom) and the left large deviation tails via a replica calculation are two of the most important unsolved issues in the field.

2. As in every replica calculation, in order to make further progress we need to exchange the natural order of limits, and go for $N \gg 1$ first (before taking the double-scaling $(\tilde{\beta}, n)$ limit as per Eq. (97)).

3. The replica framework developed here has the advantage of not needing the joint probability density of *eigenvalues*, which is actually not known for a large class of random matrices. Only the joint probability density of the *entries* is needed (of course along with our ability to compute explicit averages over it, as we did in Eq. (98) for the Gaussian case).

Eq. (119) lends itself to a saddle-point approximation for large N, which we need to take first. This leads to

$$\left\langle \left[Z_N^{(H)}(\tilde{\beta})\right]^n \right\rangle_H \approx \mathrm{e}^{NS[Q_{extr}]} \ , \tag{121}$$

where the matrix Q_{extr} is determined via the saddle point equations

$$\left.\frac{\partial S}{\partial Q_{ab}}\right|_{Q=Q_{extr}} = 0 \Rightarrow \frac{\tilde{\beta}^2}{4} Q_{ab} + \frac{1}{2} [Q^{-1}]_{ba} = 0 \qquad a > b \ , \tag{122}$$

where we have again used the log-det identity in Appendix V B.

We now make a so-called *replica-symmetric ansatz* for the structure of the matrix Q_{extr}, which extremizes the action $S[Q]$, namely we assume that all replicas are created equal, and Q_{extr} takes up the form

$$Q_{extr} = \begin{pmatrix} 1 & q & \cdots & q \\ q & 1 & \cdots & q \\ \vdots & \vdots & \ddots & \vdots \\ q & q & \cdots & 1 \end{pmatrix} \ , \tag{123}$$

depending on a single off-diagonal parameter $0 \leq q \leq 1$, where the last condition is necessary to ensure that the matrix be positive semi-definite. We indeed apply here an extended version of the Sylvester's criterion [102] that states that a symmetric matrix is positive semi-definite if and only if all its *principal minors*[16] are nonnegative. This results in the conditions

$$1-q\geq 0 \qquad \text{and} \qquad \frac{1}{1-n}\leq q\leq 1\ . \tag{124}$$

Given that – at this stage – the size of the matrix is an *arbitrary* integer, it follows that we should restrict the value q of the off-diagonal entries to the range $0\leq q\leq 1$.

We now make the following ansatz for its inverse

$$Q_{extr}^{-1}=\begin{pmatrix} \gamma & & & & \\ & \gamma & & \Large\eta & \\ & & \ddots & & \\ & \Large\eta & & \gamma & \\ & & & & \gamma \end{pmatrix}\ . \tag{125}$$

It follows that

$$[Q_{extr}Q_{extr}^{-1}]_{aa}=\gamma+(n-1)q\eta \tag{126}$$
$$[Q_{extr}Q_{extr}^{-1}]_{ab}=q\gamma+\eta+(n-2)q\eta\ , \tag{127}$$

which should be set to 1 and 0, respectively. Solving for γ and η, we find

$$\gamma=\frac{1+q(n-2)}{(1-q)(1+q(n-1))} \tag{128}$$
$$\eta=\frac{-q}{(1-q)(1+q(n-1))}\ . \tag{129}$$

Therefore the saddle-point equations (122) for the off-diagonal elements reduce to

$$\boxed{\frac{\tilde{\beta}^2}{4}q-\frac{1}{2}\frac{q}{(1-q)(1+q(n-1))}=0}\ . \tag{130}$$

Evaluating now the action (120) at the saddle point

$$S[Q_{extr}]=\frac{\tilde{\beta}^2}{8}\left[n+n(n-1)q^2\right]+\frac{1}{2}(n-1)\log(1-q)+\frac{1}{2}\log(1+(n-1)q)\ , \tag{131}$$

where we used that

$$\det_{n\times n}\begin{pmatrix} \gamma & & & & \\ & \gamma & & \Large\eta & \\ & & \ddots & & \\ & \Large\eta & & \gamma & \\ & & & & \gamma \end{pmatrix}=(\gamma-\eta)^{n-1}[\gamma+(n-1)\eta] \tag{132}$$

(formula left as an exercise), resulting in

$$\det Q_{extr}=(1-q)^{n-1}(1+(n-1)q)\ . \tag{133}$$

Apart from the trivial solution $q=0$, Eq. (130) admits another solution from

$$(1-q)(1+q(n-1))=\frac{2}{\tilde{\beta}^2}\Rightarrow(1-n)q^2+(n-2)q+1-\frac{2}{\tilde{\beta}^2}=0 \tag{134}$$

---

[16] A principal minor of a matrix is the determinant of the sub-matrix obtained by erasing corresponding sets of rows and columns (e.g. rows 1 and 6, and columns 1 and 6).

with discriminant

$$\Delta = (n-2)^2 - 4(1-n)(1-2/\tilde{\beta}^2) , \tag{135}$$

which becomes (after setting $n = -s/\tilde{\beta}$)

$$\Delta = (n-2)^2 - 4(1-n)(1-2/\tilde{\beta}^2) = \frac{\tilde{\beta}\left(s^2+8\right)+8s}{\tilde{\beta}^3} . \tag{136}$$

Therefore, the values for q that solve Eq. (134) are

$$q_{1,2} = \frac{2-n \pm \sqrt{\frac{\tilde{\beta}(s^2+8)+8s}{\tilde{\beta}^3}}}{2(1-n)} = \frac{2+(s/\tilde{\beta}) \pm \sqrt{\frac{\tilde{\beta}(s^2+8)+8s}{\tilde{\beta}^3}}}{2(1+s/\tilde{\beta})} \approx 1 + \frac{\pm\sqrt{s^2+8}-s}{2\tilde{\beta}} + \mathcal{O}(1/\tilde{\beta}^2) , \tag{137}$$

where I used the Taylor expansion for $\tilde{\beta} \to \infty$

$$\left(1+\frac{A}{\tilde{\beta}}\right)^b \sim 1 + \frac{Ab}{\tilde{\beta}} + \frac{A^2 b(b-1)}{2\tilde{\beta}^2} + \ldots \tag{138}$$

One of the roots $q_{1,2}$ is > 1 (in the $\tilde{\beta} \gg 1$ limit and for $s < 0$) and should be discarded, as it would yield a non-positive-definite matrix Q_{extr}. The other is the physically relevant one and should be kept

$$q^\star = 1 - v(s)\frac{1}{\tilde{\beta}} + \mathcal{O}(1/\tilde{\beta}^2) , \tag{139}$$

with

$$v(s) = \frac{1}{2}(\sqrt{s^2+8}+s) . \tag{140}$$

Inserting this value into the action (131) with $n = -s/\tilde{\beta}$ yields

$$\begin{aligned} S[Q_{extr}] &= \frac{\tilde{\beta}^2}{8}\left[-\frac{s}{\tilde{\beta}} - \frac{s}{\tilde{\beta}}(-s/\tilde{\beta}-1)\left(1-v(s)\frac{1}{\tilde{\beta}}\right)^2\right] + \frac{1}{2}(-s/\tilde{\beta}-1)\log(v(s)/\tilde{\beta}) + \frac{1}{2}\log(1+(-s/\tilde{\beta}-1)(1-v(s)(1/\tilde{\beta}))) \\ &\approx -\frac{s}{8}(2v(s)-s) - \frac{1}{2}\log v(s) + \frac{1}{2}\log(v(s)-s) , \end{aligned} \tag{141}$$

in the limit $\tilde{\beta} \to \infty$.

Re-tracing the various steps from Eq. (97) and (121)

$$\left\langle \exp\left(-s\frac{N}{2}\lambda_1\right)\right\rangle_H = \lim_{\tilde{\beta}\to\infty}\left\langle\left[Z_N^{(H)}(\tilde{\beta})\right]^{-s/\tilde{\beta}}\right\rangle_H \approx \exp\left[N\left(-\frac{s}{8}(2v(s)-s) - \frac{1}{2}\log v(s) + \frac{1}{2}\log(v(s)-s)\right)\right] , \tag{142}$$

which can be written explicitly as

$$\int \mathrm{d}x\ f_{r_1}(x)\mathrm{e}^{-s\frac{N}{2}x} \approx \mathrm{e}^{N\phi(s)} , \tag{143}$$

where $f_{r_1}(x)$ is the probability density function of the largest eigenvalue of the GOE, and

$$\begin{aligned} \phi(s) &= -\frac{s}{8}(2v(s)-s) - \frac{1}{2}\log v(s) + \frac{1}{2}\log(v(s)-s) \\ &= \frac{1}{8}\left(-s\sqrt{s^2+8} + 4\log\left(\sqrt{s^2+8}-s\right) - 4\log\left(\sqrt{s^2+8}+s\right)\right) . \end{aligned} \tag{144}$$

Assuming for $f_{r_1}(x)$ the large deviation form $f_{r_1}(x) \approx \exp(-N\Phi_+(x))$ – which we know is only valid for anomalous fluctuations to the *right* of its expected value – and evaluating the integral on the l.h.s. using the Laplace approximation, we get

$$\int \mathrm{d}x\ f_{r_1}(x)\mathrm{e}^{-s\frac{N}{2}x} \approx \int \mathrm{d}x\ \mathrm{e}^{-N\left[\Phi_+(x)+\frac{s}{2}x\right]} \approx \exp\left[-N\min_x\left[\Phi_+(x)+\frac{s}{2}x\right]\right] . \tag{145}$$

Comparing (143) with (145), we can write (see [1] for details on the Legendre-Fenchel method to recover the large deviation function in real space from that in Laplace space)

$$\phi(s) = -\min_x \left[\Phi_+(x) + \frac{s}{2}x\right] \ . \tag{146}$$

It now remains to check that Eq. (146) holds for $\Phi_+(x)$ given by the Majumdar-Vergassola formula (41)

$$\Phi_+(x) = \frac{1}{2}x\sqrt{x^2-2} + \log\left(\frac{x-\sqrt{x^2-2}}{\sqrt{2}}\right) \ . \tag{147}$$

If this were the case, we would have shown that the outcome of a replica calculation (the function $\phi(s)$ on the l.h.s. (146)) indeed matches the result obtained for the large deviation function from a Coulomb gas physical analogy (the function on the r.h.s. of (146)).

The value $x^\star(s)$ that minimizes the term in square brackets in (146) is given by

$$\Phi_+'(x^\star(s)) + s/2 = 0 \Rightarrow \frac{s}{2} + \frac{x^\star(s)^2}{2\sqrt{x^\star(s)^2-2}} + \frac{\sqrt{x^\star(s)^2-2}}{2} + \frac{1-\frac{x^\star(s)}{\sqrt{x^\star(s)^2-2}}}{x^\star(s)-\sqrt{x^\star(s)^2-2}} = 0 \ , \tag{148}$$

which can be massively simplified into (note that $s<0$)

$$\frac{s}{2} + \sqrt{x^\star(s)^2-2} = 0 \ , \tag{149}$$

giving (selecting the positive root as $x^\star(s) > \sqrt{2}$ represent fluctuations of the largest eigenvalue to the *right* of its expected value)

$$x^\star(s) = \frac{1}{2}\sqrt{s^2+8} \ . \tag{150}$$

Therefore the relation we have to prove from (146) is

$$\frac{1}{8}\left(-s\sqrt{s^2+8} + 4\log\left(\sqrt{s^2+8}-s\right) - 4\log\left(\sqrt{s^2+8}+s\right)\right) \stackrel{?}{=} -\Phi_+(x^\star(s)) - (s/2)x^\star(s) \ , \tag{151}$$

which can be verified after a bit of tedious algebra. Eq. (146) can also be verified directly in Mathematica using the following code (see Fig. 8). I leave as an exercise to derive $\Phi_+(x)$ from scratch from Eq. (146) by inverting the Legendre transform. The remaining big challenge is to obtain the Tracy-Widom law for typical fluctuations, as well as the *left* large deviation function describing fluctuations of $\mathcal{O}(N^2)$, via a replica calculation. This remains an outstanding puzzle.

```
Clear[Phiplus, v, s];
(* Majumdar-Vergassola right large deviation function *)

Phiplus[x_] := x/2 Sqrt[x^2 - 2] + Log[(x - Sqrt[x^2 - 2])/Sqrt[2]];

(* Find the Legendre-Fenchel minimum (r.h.s. of Eq. (146)) *)

LegendreMin =
  Table[{-s, -FindMinimum[Phiplus[x] + (-s/2) x, {x, 3}][[1]]}, {s, 1,
     100, 5}];

(* L.h.s. of Eq. (146) - obtained via replica *)

v[s_] := (1/2) (s + Sqrt[s^2 + 8]);
\[Phi][s_] := -(s/8)*(2 v[s] - s) - (1/2) Log[v[s]] + (1/2) Log[v[s] - s];

(* Plot of l.h.s. and r.h.s. *)
Plot1 = ListPlot[LegendreMin, PlotStyle -> {Red, PointSize[Large]}];
Plot2 = Plot[\[Phi][s], {s, -100, 0}, PlotStyle -> {Blue, Thick}];
Show[
 Plot1, Plot2,
 AxesLabel -> {Style["s", Larger], None},
 Ticks -> {Automatic, None},
 PlotRange -> All,
 GridLines -> None
]
```

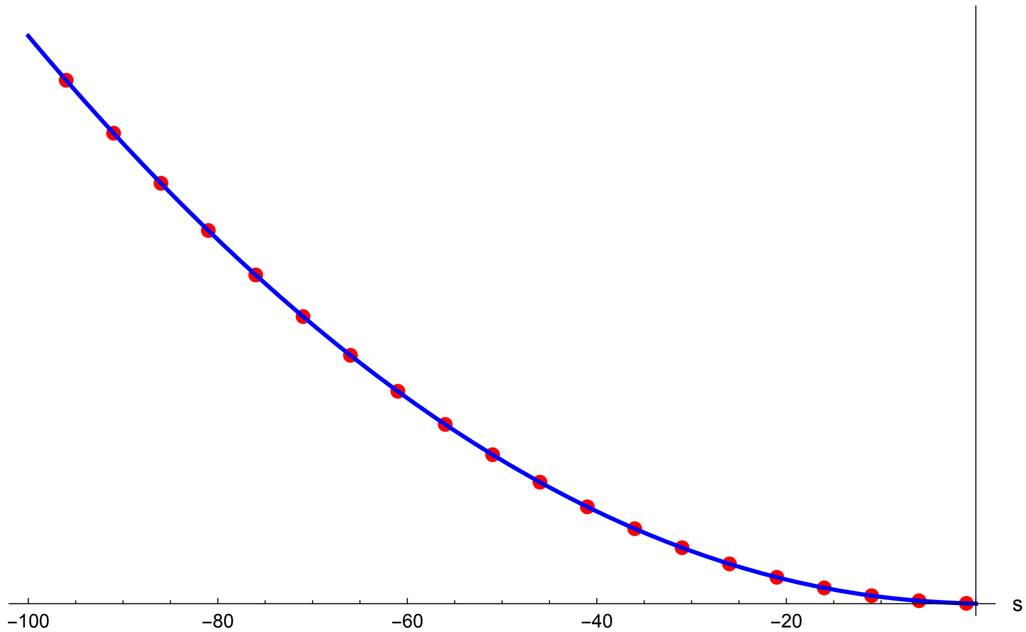

FIG. 8. Numerical check of Eq. (146) in Mathematica. Solid blue line is the replica result $\phi(s)$. Red dots correspond to the numerical minimization of the r.h.s. of (146), where $\Phi_+(x)$ is the Majumdar-Vergassola formula (41) obtained via a Coulomb gas method.

A. Appendix: Laplace method for the asymptotic evaluation of integrals

The Laplace method is a powerful technique used in the field of asymptotic analysis for approximating integrals. This method is particularly useful when dealing with integrals that are difficult to evaluate using standard techniques. The Laplace method is based on the principle of approximating the integral of an exponentially decaying function by the function's value at its extremal point(s).

Consider an integral of the form

$$I(T) = \int_a^b \mathrm{e}^{Tf(x)} g(x)\,\mathrm{d}x, \tag{152}$$

where T is a large parameter, and $f(x)$ and $g(x)$ are smooth functions. The objective is to find an asymptotic approximation of $I(T)$ as $T \to \infty$.

The Laplace method is based on the observation that, for large T, the main contribution to the integral comes from the neighbourhood of the point where $f(x)$ attains its maximum value inside the interval (a, b). Assume this maximum occurs at a point $x_0 \in (a, b)$ such that $f''(x_0) < 0$.

Expanding $f(x)$ around x_0 using Taylor's theorem, we get

$$f(x) \approx f(x_0) + \frac{1}{2} f''(x_0)(x - x_0)^2 + \dots\ , \tag{153}$$

where we used the fact that $f'(x_0) = 0$ being a maximum. We can also similarly expand the function $g(x)$ to get

$$g(x) \approx g(x_0) + g'(x_0)(x - x_0) + \dots\ . \tag{154}$$

Substituting these expansions into the integral, and keeping only the first terms, we obtain

$$I(T) \approx \mathrm{e}^{Tf(x_0)} g(x_0) \int_a^b \mathrm{e}^{-\frac{1}{2}T|f''(x_0)|(x-x_0)^2} \left[1 + \frac{g'(x_0)}{g(x_0)}(x - x_0) + \dots\right] \mathrm{d}x\ . \tag{155}$$

Making a change of variables $\sqrt{T}(x - x_0) = y$, we get

$$I(T) \approx \mathrm{e}^{Tf(x_0)} g(x_0) \int_{-\sqrt{T}(x_0-a)}^{\sqrt{T}(b-x_0)} \mathrm{e}^{-\frac{1}{2}|f''(x_0)|y^2} \left[1 + \frac{g'(x_0)}{g(x_0)} \frac{y}{\sqrt{T}} + \dots\right] \mathrm{d}y\ . \tag{156}$$

For large T, the exponential function rapidly decays away from x_0, allowing us to extend the limits of integration to infinity. Ignoring also the sub-leading terms in square brackets, we get to leading order for large T

$$I(T) \approx \mathrm{e}^{Tf(x_0)} g(x_0) \int_{-\infty}^{\infty} \mathrm{e}^{-\frac{1}{2}|f''(x_0)|y^2}\, \mathrm{d}y = \mathrm{e}^{Tf(x_0)} g(x_0) \sqrt{\frac{2\pi}{T|f''(x_0)|}} \ , \tag{157}$$

where we have evaluated the Gaussian integral exactly.

B. Appendix: derivative of Log-Det identity (used in Eqs. (116) and (122))

We give here a proof of the identity (assuming $\det M > 0$)

$$\boxed{\frac{\partial}{\partial M_{ab}} \log\det M = [M^{-1}]_{ba}} \ . \tag{158}$$

Proof: By the chain rule

$$\frac{\partial}{\partial M_{ab}} \log\det M = \frac{1}{\det M} \frac{\partial}{\partial M_{ab}} \det M \ . \tag{159}$$

Using the cofactor expansion of the determinant along the a-th row

$$\det M = \sum_{k=1}^{n} M_{ak} C_{ak} \ , \tag{160}$$

where the cofactor matrix C is

$$C_{ij} = (-1)^{i+j} T_{ij} \tag{161}$$

and T_{ij} is a *minor* of M, i.e. the determinant of the $(n-1)\times(n-1)$ matrix obtained removing the i-th row and j-th column of M.

Hence

$$\frac{\partial}{\partial M_{ab}} \det M = \sum_{k=1}^{n} \left[\underbrace{\frac{\partial M_{ak}}{\partial M_{ab}}}_{\delta_{kb}} C_{ak} + M_{ak} \underbrace{\frac{\partial C_{ak}}{\partial M_{ab}}}_{=0} \right] \ , \tag{162}$$

where the last term vanishes as the elements in row a do not affect the corresponding cofactor.

It follows from (159) and (162) that

$$\frac{\partial}{\partial M_{ab}} \log\det M = \frac{C_{ab}}{\det M} = \frac{[\mathrm{adj}(M)]_{ba}}{\det M} \ , \tag{163}$$

where we use the fact that the adjugate matrix $\mathrm{adj}(M)$ is the transpose of the cofactor matrix. The right hand side of (163) is readily recognised as the element ba of the inverse matrix of M.

For symmetric M, this identity provides an integral representation for an entry of the inverse matrix M^{-1} as an interesting corollary. Indeed we have

$$\begin{aligned}
[M^{-1}]_{ba} &= \frac{\partial}{\partial M_{ab}} \log\det M = (-2)\frac{\partial}{\partial M_{ab}} \log(\det M)^{-1/2} = (-2)\frac{\partial}{\partial M_{ab}} \log \int_{\mathbb{R}^n} \mathrm{d}^n x\ \mathrm{e}^{-\frac{1}{2}\vec{x}^T M \vec{x}} \\
&= \frac{\int_{\mathbb{R}^n} \mathrm{d}^n x\ x_a x_b \mathrm{e}^{-\frac{1}{2}\vec{x}^T M \vec{x}}}{\int_{\mathbb{R}^n} \mathrm{d}^n x\ \mathrm{e}^{-\frac{1}{2}\vec{x}^T M \vec{x}}} \ ,
\end{aligned} \tag{164}$$

where we have used the Gaussian integral formula given in footnote 12 (provided the integrals are convergent).

VI. LECTURE 4/5 - PUSHED PHASE: SPECTRAL RADIUS FOR GENERAL CONFINING POTENTIAL $V(x)$

In these two lectures, we start again from the real log-gas joint probability density (18)

$$\mathcal{P}_{\beta,N}(x_1,\dots,x_N)=\frac{1}{\mathcal{Z}_{N,\beta}}\mathrm{e}^{-\beta E(x_1,\dots,x_N)}\ , \tag{165}$$

$$E(x_1,\dots,x_N)=-\frac{1}{2}\sum_{i\neq j}\log|x_i-x_j|+N\sum_k V(x_k)\ , \tag{166}$$

this time keeping the potential sufficiently general (i.e. not restricted to Gaussian). We focus here on the *spectral radius*

$$r_2=\max_j|x_j| \tag{167}$$

and ask whether the cumulative distribution $\mathrm{Prob}[r_2\leq R]$ can be characterized in the large deviation sense. The derivation of a general formula for the large deviation function (excess free energy) $F(R)$ follows very closely the paper [30]. We consider potentials $V(x)$ satisfying the following assumption.

Assumption 1: $V(x)$ is $C^3(\mathbb{R})$, symmetric $V(x)=V(-x)$, strictly convex and satisfies $\liminf_{|x|\to\infty}\frac{V(x)}{\log|x|}>1$.

We remark that strictly convex and super-logarithmic $V(x)$'s are in the class of so-called *one-cut, off-critical* potentials – namely, potentials for which the average spectral density is supported on a single interval on the real line, and decays as a square root at the upper edge $R_\star$ (like the semicircle for Gaussian ensembles).

In the large-N limit, the eigenvalue empirical measure $n(x)=\frac{1}{N}\sum_i\delta_{x,x_i}$ weakly converges to a deterministic density[17] $n^\star_{R_\star}(x)$. This limit is the *equilibrium measure* (the minimizer) of the energy functional

$$\mathcal{E}[n(x)]=-\frac{1}{2}\iint_{\mathbb{R}\times\mathbb{R}}\log|x-y|\mathrm{d}n(x)\mathrm{d}n(y)+\int_{\mathbb{R}}V(x)\mathrm{d}n(x)\ . \tag{168}$$

An electrostatic derivation of this fact will be presented in the next sub-section.

For concreteness, let us focus on the Gaussian Unitary Ensemble (GUE) defined by the measure (18) with $V(x)=x^2/2$ and $\beta=2$. In this case, the equilibrium measure is supported on the symmetric interval $[-R_\star,R_\star]$ where $R_\star=\sqrt{2}$, with the Wigner semicircular density Eq. (24). Moreover, as $N\to\infty$, the extreme statistics $r_2=\max_j|x_j|$ converges to the edge $R_\star$, namely $\mathrm{Prob}\left(\max_j|x_j|\leq R\right)$ converges to a step function: 0 if $R<R_\star$, and 1 if $R>R_\star$. For large N, the fluctuations of the spectral radius $r_2=\max_j|x_j|$ around $R_\star$ over the typical scale $\mathcal{O}(N^{-2/3})$ are described by a *squared Tracy-Widom distribution*. In formulae [103, 104],

$$\lim_{N\to\infty}\mathrm{Prob}\left[\max_j|x_j|\leq R_\star+\frac{t}{\sqrt{2}N^{2/3}}\right]=\mathcal{F}_2^2(t)\ , \tag{169}$$

where $\mathcal{F}_\beta(t)$ is the β-Tracy-Widom distribution (32). The macroscopic (atypical) fluctuations of $r_2=\max_j|x_j|$ are instead described by a large deviation function. More precisely, for all $\beta>0$ the following limit exists

$$-\lim_{N\to\infty}\frac{1}{\beta N^2}\log\mathrm{Prob}\left[\max_j|x_j|\leq R\right]=-\lim_{N\to\infty}\frac{1}{\beta N^2}\log\frac{Z_N(R)}{Z_N(\infty)}=F(R)\ , \tag{170}$$

in complete analogy with Eq. (46), where this time

$$Z_N(R)=\int_{-R}^{R}\cdots\int_{-R}^{R}\mathrm{d}x_1\cdots\mathrm{d}x_N\ \mathrm{e}^{-\beta E(x_1,\dots,x_N)}\ . \tag{171}$$

In physical term, $Z_N(R)$ is the canonical partition function at inverse temperature β of a log-gas on a line, subject to a confining potential $V(x)$ and constrained to lie within two hard "walls" at $-R$ and R. The denominator is nothing but the partition function of the same gas when the constraining walls are released to $\pm\infty$. The quantity $F(R)$ therefore represents the *excess free energy* of the gas (at zero temperature), which essentially measure the level of discomfort the gas particles will feel in being squeezed within a much narrower region (the interval $[-R,R]$) than they would normally occupy at equilibrium.

The general picture is as follows (see Fig. 9):

---

[17] For the Gaussian confining potential $V(x)=x^2/2$, this would be the semicircle law, $n^\star_{R_\star}(x)=\varrho_{\mathrm{sc}}(x)$.

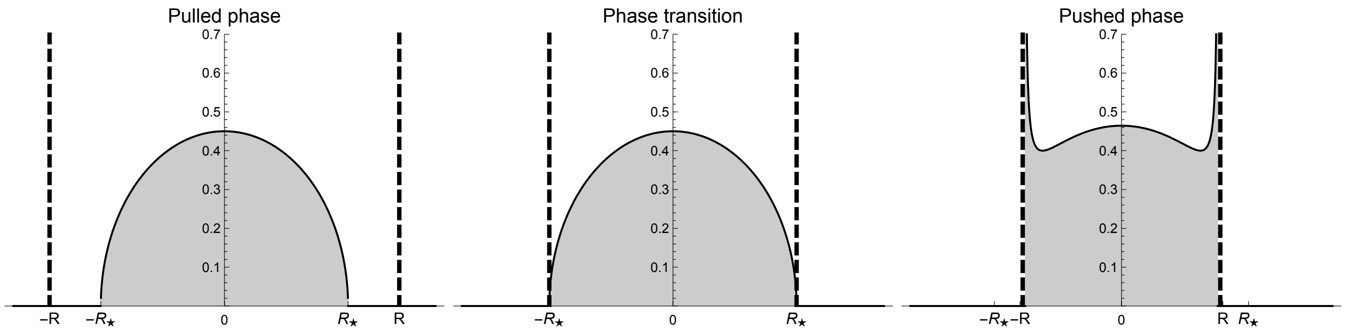

FIG. 9. The pulled-to-pushed transition for a log-gas in dimension $d = 1$ in a quadratic potential (GUE). Figure taken from [30].

i) If $R > R_\star$, the wall constraint is immaterial, and hence the equilibrium density of the gas is a certain function $n^\star_{R_\star}(x)$, which minimizes the energy functional (168) over the entire real. This is the so-called *pulled phase*, borrowing a terminology suggested in [64]. In this phase, the excess free energy is $F(R) = 0$.

ii) If $R < R_\star$ the system is in a *pushed phase*, the constraint is effective, and the equilibrium energy of the system increases, leading to $F(R) > 0$.

iii) At $R = R_\star$ the gas undergoes a *phase transition* and the excess free energy $F(R)$ displays a non-analytic behavior.

Explicitly solvable models related to random matrices suggest that in the vicinity of the critical point

$$F(R) \simeq (R_\star - R)^3 \mathbb{1}_{R \le R_\star} \ , \tag{172}$$

implying that the transition between the *pushed* and *pulled* phases of the gas is third-order. In [30], we demonstrated that (172) is generically true for a large class of systems with repulsive interactions.

The calculation of $F(R)$ for the GUE (hereafter called $F_{\mathrm{GUE}}(R)$) and its $\beta > 0$ extensions was performed in detail by Dean and Majumdar [58] and essentially reproduced in detail in the next subsection. They found explicit expressions for the equilibrium density of the gas

$$n^\star_R(x) = \begin{cases} \dfrac{1}{\pi} \dfrac{2 + R^2 - 2x^2}{2\sqrt{R^2 - x^2}} \mathbb{1}_{|x|<R} & \text{if } R < R_\star \text{ (pushed phase)} \\ \dfrac{1}{\pi} \sqrt{2 - x^2} \mathbb{1}_{|x| \le R_\star} & \text{if } R \ge R_\star \text{ (pulled phase)} \ , \end{cases} \tag{173}$$

and for the excess free energy

$$F_{\mathrm{GUE}}(R) = \begin{cases} \dfrac{1}{32} \left(8R^2 - R^4 - 16 \log R - 12 + 8 \log 2 \right) & \text{if } R < R_\star \\ 0 & \text{if } R \ge R_\star \ . \end{cases} \tag{174}$$

As remarked earlier, we see that

$$F_{\mathrm{GUE}}(R) \sim \frac{1}{3\sqrt{2}} (R_\star - R)^3 \mathbb{1}_{R \le R_\star} \ , \tag{175}$$

as $R \to R_\star$. Therefore, the third derivative of the free energy of the log-gas at the critical point $R_\star = \sqrt{2}$ is discontinuous.

Similar phase transitions of the pulled-to-pushed type have been observed in several physics models related to random matrices [28, 105], including large-N gauge theories [106–109], longest increasing subsequences of random permutations [110], quantum transport fluctuations in mesoscopic conductors [111–115], non-intersecting Brownian motions [50, 116], entanglement measures in a bipartite system [117–120], random tilings [121, 122], random landscapes [123], and the tail analysis in the KPZ problem [124]. (See also the recent popular science articles [125, 126].)

An explanation of the critical exponent '3' for the largest eigenvalue r_1 (even though their argument would work for r_2 as well) has been put forward by Majumdar and Schehr [28] based on a standard extreme value statistics criterion and a matching argument of the large deviation function behavior in the vicinity of the critical value $R_\star$ and the left tail of the limiting distribution for typical fluctuations. I reproduce their argument here.

Let, in general, $n^\star_{R_\star}(x) \sim (R_\star - x)^\gamma$ at the upper soft edge $x = R_\star$. One can easily estimate the scale of typical fluctuation δr_1 of r_1 around its mean $R_\star$. Using the standard EVS criterion (see footnote 1), one gets (exercise)

$$\delta r_1 = R_\star - r_1 \sim \mathcal{O}(N^{-1/(1+\gamma)}) . \tag{176}$$

For $\gamma = 1/2$ (valid for the semicircle law and in general for *off-critical* ensembles), one indeed recovers $\delta r_1 \sim \mathcal{O}(N^{-2/3})$. Hence, one would expect that on this scale, the Cumulative Distribution Function of r_1 will have the scaling form (cf. Eq. (30))

$$\mathrm{Prob}[r_1 \leq w] \sim \mathcal{F}\left(N^{1/(1+\gamma)}(w - R_\star)\right) , \tag{177}$$

where the scaling function $\mathcal{F}(x)$ is the γ-analogue of the Tracy-Widom law (32). Now, in general, we would expect that far in the left tail, this function should decay asymptotically as,

$$\mathcal{F}(x) \sim \exp[-a_0\,|x|^\delta] \text{ , for } x \to -\infty , \tag{178}$$

where a_0 is a constant. Clearly, for $\gamma = 1/2$ case (i.e., when $\mathcal{F}(x)$ is the standard Tracy-Widom), one has $\delta = 3$ (see Eq. (34)).

On the other hand, it follows from a general Coulomb gas argument (see detailed treatment below) that atypical fluctuations of r_1 of $\sim \mathcal{O}(1)$ to the left of $R_\star$, i.e., when $w < R_\star$, are described by a large deviation form

$$\mathrm{Prob}[r_1 \leq w] \sim \exp\left[-\beta\, N^2 \Phi_-(w)\right] , \quad w < R_\star , \tag{179}$$

where $\Phi_-(w)$ is a rate function that should vanish as $w \to R_\star$ from the left. Interpreting $\Phi_-(w)$ as the excess free energy of the gas in the pushed phase, we then expect $\Phi_-(w) \sim a_1\,(R_\star - w)^\sigma$ as $w \to R_\star$ where a_1 is a constant and the exponent σ then decides the order of the transition. To estimate σ, we match this left large deviation results (when $w \to R_\star$) with the extreme left tail of the central peak region as described in (178).

Recall: *The most unlikely of typical fluctuations should smoothly match the most likely of atypical fluctuations.*

Substituting $\Phi_-(w) \sim a_1\,(R_\star - w)^\sigma$ in (179) gives, for $w \to R_\star$,

$$\begin{aligned} \mathrm{Prob}[r_1 \leq w] &\sim \exp\left[-\beta\, N^2\, a_1\,(R_\star - w)^\sigma\right] , \\ &\sim \exp\left[-\beta\, a_1\, \left[N^{2/\sigma}\,(R_\star - w)\right]^\sigma\right] . \end{aligned} \tag{180}$$

In contrast, for $(R_\star - w) \gg N^{-1/(1+\gamma)}$, we get, by using the left tail asymptotics (178) of the central peak behavior in (177),

$$\mathrm{Prob}[r_1 \leq w] \sim \exp\left[-a_0\left\{N^{1/(1+\gamma)}\,(R_\star - w)\right\}^\delta\right] . \tag{181}$$

Assuming that the two behaviors merge smoothly, we find by comparing (180) and (181)

$$\delta = \sigma \text{ and } \frac{\delta}{1+\gamma} = 2 , \tag{182}$$

which then relates the order of the transition σ to the exponent γ characterizing the vanishing of the charge density at the soft edge, via the simple scaling relation

$$\sigma = 2\,(1+\gamma) . \tag{183}$$

For example, for $\gamma = 1/2$, one recovers the third order transition $\sigma = 3$. As an example, a 'critical' potential whose equilibrium density decays with an exponent $\gamma = 5/2$ at the upper edge $R_\star$, will then have a seventh order ($\sigma = 7$) phase transition.

The criterion predicts that if the equilibrium density of a log-gas in the pulled phase vanishes as $n^\star_{R_\star}(x) \sim \sqrt{R_\star^2 - x^2}$ at the edges – the so-called *off-critical* case – then the pulled-to-pushed phase transition is of the third order. This conjectural relation between the particular behavior of the gas density and the arising non-analyticities in the free energies has been verified in several examples, even though each particular case (i.e. each matrix ensemble defined by a potential V) requires working out explicitly the model-dependent $F(R)$ to compute the critical exponent. I show later that a general formula for $F(R)$ can be obtained for arbitrary confining potential satisfying **Assumption 1**, which incidentally proves the universality of the third-order phase transition for one-cut, off-critical matrix models and confirms the heuristic Majumdar-Schehr criterion.

A. Electrostatic derivation of the energy functional (168)

Consider the N-fold integral (171)

$$Z_N(R) = \int_{-R}^{R} \cdots \int_{-R}^{R} \mathrm{d}x_1 \cdots \mathrm{d}x_N \ \mathrm{e}^{-\beta E(x_1,\ldots,x_N)} \ , \tag{184}$$

where

$$E\left(x_1,\ldots,x_N\right) = -\frac{1}{2}\sum_{i\neq j} \log|x_i - x_j| + N\sum_k V\left(x_k\right) \tag{185}$$

and $V(x)$ satisfies **Assumption 1**.

We may now derive a continuous field theory for the problem, where the individual charge locations $\{x_i\}$ are replaced by a continuous density of charge. To this end, we introduce the empirical density

$$n_R(x) = \frac{1}{N}\sum_i \delta_{x,x_i} \ , \tag{186}$$

which counts how many charged particles are there at location x within $[-R, R]$. We further assume that for large N, $n_R(x)$ will converge to a non-negative, sufficiently regular, and normalized function of the position x.

We can now enforce the definition (186) via a functional delta integration over non-negative, regular, and normalized functions as

$$1 = \int \mathcal{D}[n_R(x)]\delta\left[n_R(x) - \frac{1}{N}\sum_i \delta_{x,x_i}\right] \ . \tag{187}$$

Inserting this identity (see [127] for details on functional integration) into the multiple integral (184), and using the identities

$$\sum_i f(x_i) = N\int \mathrm{d}x\ n_R(x) f(x) \tag{188}$$

$$\sum_{i,j} g(x_i, x_j) = N^2 \iint \mathrm{d}x\mathrm{d}x' n_R(x) n_R(x') g(x,x') \ , \tag{189}$$

we can express the two terms in the energy (185) as

$$N\sum_k V\left(x_k\right) = N^2 \int \mathrm{d}x\ n_R(x) V(x) \tag{190}$$

$$\begin{aligned} -\frac{1}{2}\sum_{i\neq j}\log|x_i - x_j| &= -\frac{1}{2}\left[\sum_{i,j}\log|x_i - x_j| - \sum_i \log\Delta(x_i)\right] \\ &= -\frac{1}{2}\left[N^2 \iint \mathrm{d}x\mathrm{d}x' n_R(x) n_R(x') \log|x - x'| - N\int \mathrm{d}x\ n_R(x)\log\Delta(x)\right] \ , \end{aligned} \tag{191}$$

where in the second line we have added and subtracted the infinite self-energy contribution that arises when two neighboring particles sitting around the point x attain a vanishing separation $\Delta(x)$. Dyson [4] gave a heuristic argument for $\Delta(x)$ having the form $\Delta(x) \approx c/(N n_R(x))$, based on the consideration that the higher the density of particles around position x the smaller the inter-particle separation – note, however, that this simplistic argument would not fix the constant c. There has been an impressive amount of work done in recent times (see e.g. [128, 129] and references therein) to characterize rigorously the next-to-leading order in the approximation of the discrete-charge energy functional and to take good care of the self-energy term. Fortunately, we do not need very sophisticated considerations if we confine ourselves to the leading order term.

Eventually, the multiple integral defining $Z_N(R)$ in (184) can be rewritten (exchanging orders of integration) as

$$\begin{aligned} Z_N(R) \approx \int \mathcal{D}[n_R(x)] \exp\Bigg[-\beta N^2 \Bigg(\int \mathrm{d}x\ n_R(x) V(x) - \frac{1}{2}\iint \mathrm{d}x\mathrm{d}x' n_R(x) n_R(x') \log|x - x'| \\ + \frac{1}{2N}\int \mathrm{d}x\ n_R(x)\log\Delta(x)\Bigg)\Bigg] \times \int_{-R}^{R} \cdots \int_{-R}^{R} \mathrm{d}x_1 \cdots \mathrm{d}x_N \delta\left[n_R(x) - \frac{1}{N}\sum_i \delta_{x,x_i}\right] \ . \end{aligned} \tag{192}$$

In physical terms, what we have done is as follows. Instead of summing over the "microstates" (individual configurations of charges), we first fix a certain charge density profile $n_R(x)$ (non-negative, regular, and normalized). Then, we sum over all microstates "compatible" with $n_R(x)$ (as signalled by the last multiple integral in (192)). Finally, we sum over all possible (non-negative, regular, and normalized) functions $n_R(x)$.

The term

$$\Psi[n_R(x)] = \int_{-R}^{R} \cdots \int_{-R}^{R} \mathrm{d}x_1 \cdots \mathrm{d}x_N \delta \left[n_R(x) - \frac{1}{N} \sum_i \delta_{x,x_i} \right] \tag{193}$$

indeed counts how many microstates exist that are compatible with a given $n_R(x)$. Dean and Majumdar [58] have shown that for large N, the term $\Psi[n_R(x)]$ indeed has an "entropy" form given by

$$\Psi[n_R(x)] \approx \exp\left[-N \int \mathrm{d}x \; n_R(x) \log n_R(x) \right] \; . \tag{194}$$

I will reproduce their derivation in the appendix VI B.

Fortunately, both the self-energy and the entropy terms are sub-leading ($\mathcal{O}(N)$) with respect to the "energetic" components ($\mathcal{O}(N^2)$), hence they can be ignored for large N. From (192), one indeed deduces that for large N

$$Z_N(R) \approx \exp\left[-\beta N^2 \mathcal{E}[n_R(x)] + \mathcal{O}(N) \right] \approx \exp\left[-\beta N^2 \mathcal{E}[n_R^\star(x)] \right] \; , \tag{195}$$

where the mean-field energy functional $\mathcal{E}[\sigma]$ over the set of probability measures on $[-R, R]$ is given by

$$\mathcal{E}[\sigma] = \int_{-R}^{R} \mathrm{d}x \; \sigma(x) V(x) - \frac{1}{2} \iint_{[-R,R]^2} \mathrm{d}x \mathrm{d}x' \sigma(x) \sigma(x') \log|x - x'| \; , \tag{196}$$

while $n_R^\star(x)$ is the minimizer of this class of functionals, namely the solution of

$$\left.\frac{\delta \mathcal{E}}{\delta \sigma}\right|_{\sigma = n_R^\star} = 0 \Rightarrow \boxed{V(x) - \int_{-R}^{R} \mathrm{d}x' \; n_R^\star(x') \log|x - x'| + \mu_R = 0} \; , \tag{197}$$

for x in the support of $n_R^\star(x)$, where the *chemical potential* μ_R is a R-dependent constant that ensures normalization of the equilibrium density $\int_{-R}^{R} n_R^\star(x) \mathrm{d}x = 1$. Eq. (197) is the Euler-Lagrange equation corresponding to the mean-field energy functional $\mathcal{E}$, and it has a clear physical interpretation: the electric field felt by an infinitesimal charge at position x and generated by all other charges should perfectly balance the potential $V(x)$ generated at x by the neutralizing background. If this were not the case, charges would react to the field imbalance and spontaneously re-arrange in order not to feel any net force.

Setting now $x = Rt$ and $x' = Rt'$, and defining $\varrho_R(t) = R n_R^\star(Rt)$, we obtain after simple algebra from (197)

$$V(Rt) - \int_{-1}^{1} dt' \; \varrho_R(t') \log|t - t'| + \mu_R' = 0 \; . \tag{198}$$

This integral equation for $\varrho_R(t)$ represents an inverse electrostatic problem: contrary to the standard textbook problem of determining the potential generated at position x by the distribution of charge $\varrho(x')$ elsewhere, we here ask what distribution of charges is such that the field generated by it precisely balances the external potential elsewhere.

The integral equation can be solved by first differentiating Eq. (198) with respect to t. Since $\log|t - t'|$ is not differentiable, this requires introducing the notion of *weak derivative*. Let u be a function in $\mathcal{L}^1([a, b])$. We say that v in $\mathcal{L}^1([a, b])$ is a weak derivative of u if

$$\int_a^b \mathrm{d}x \; u(x) \varphi'(x) = -\int_a^b \mathrm{d}x \; v(x) \varphi(x) \; , \tag{199}$$

for all infinitely differentiable functions $\varphi(x)$ with $\varphi(a) = \varphi(b) = 0$. The notion of weak derivative extends the standard (strong) derivative to functions that are not differentiable, but integrable in $[a, b]$. Also, if u is differentiable in the standard sense, then its weak and strong derivatives coincide - just using integration by parts.

Setting $u(x) = \int_{-1}^{1} \mathrm{d}t' \; \varrho_R(t') \log|x - t'|$, we can write

$$\begin{aligned} &\int \varphi'(x) \left[\int_{-1}^{1} \mathrm{d}t' \; \varrho_R(t') \log|x - t'| \right] \mathrm{d}x = \frac{1}{2} \lim_{\epsilon \to 0} \int \varphi'(x) \left[\int_{-1}^{1} \mathrm{d}t' \; \varrho_R(t') \log((x - t')^2 + \epsilon^2) \right] \mathrm{d}x \\ &= -\frac{1}{2} \int \varphi(x) \left[\int_{-1}^{1} \mathrm{d}t' \; \varrho_R(t') \frac{2(x - t')}{(x - t')^2 + \epsilon^2} \right] \mathrm{d}x = -\int \varphi(x) \left[\mathrm{Pr} \int_{-1}^{1} \frac{\varrho_R(t')}{x - t'} \mathrm{d}t' \right] \mathrm{d}x \; , \end{aligned} \tag{200}$$

where Pr stands for Cauchy's principal value[18]. Comparing with (199), we see that the weak derivative of $u(x)$ is $\mathrm{Pr}\int \frac{\varrho_R(t')}{x-t'}\mathrm{d}t'$, therefore the singular integral equation to be solved is in the end

$$\mathrm{Pr}\int_{-1}^{1}\frac{\varrho_R(t')}{x-t'} = V'(Rx)\ . \tag{201}$$

This equation is of the "airfoil" (or finite Hilbert transform) type, which was considered and explicitly solved long ago by Tricomi (assuming the solution is one-cut) [130]. Applying Tricomi's formula directly, we get

$$\varrho_R(t) = \frac{1}{\pi^2\sqrt{1-t^2}}\mathrm{Pr}\int_{-1}^{1}\mathrm{d}t'\frac{\sqrt{1-t'^2}\ V'(Rt')}{t'-t} + \frac{C}{\sqrt{1-t^2}}\ , \tag{202}$$

where the constant

$$C = \frac{1}{\pi}\int_{-1}^{1}\mathrm{d}t\ \varrho_R(t) = \frac{1}{\pi} \tag{203}$$

by normalization.

Coming back to Eq. (197) and the equilibrium density $n_R^\star(t) = (1/R)\varrho_R(t/R)$, we obtain straightforwardly

$$n_R^\star(t) = \frac{P_R(t)}{\pi\sqrt{R^2-t^2}}\ , \tag{204}$$

where

$$P_R(t) = 1 - \mathrm{Pr}\int_{-R}^{R}\frac{1}{\pi}\frac{\sqrt{R^2-\tau^2}V'(\tau)}{t-\tau}\mathrm{d}\tau\ . \tag{205}$$

Note that $P_R(t)\geq 0$ to ensure that the equilibrium density is non-negative within its support. This may induce a change of shape of $n_R^\star(t)$ as R crosses over from a value $R<R_\star$ to a value $R>R_\star$, with the value of $R_\star$ depending on the external potential $V(x)$. I will not show this fact in general [131, 132], but only on the Gaussian special case, which is sufficiently instructive.

Take $V(x) = x^2/2$. Then

$$P_R(t) = 1 - \mathrm{Pr}\int_{-R}^{R}\frac{1}{\pi}\frac{\sqrt{R^2-\tau^2}\ \tau}{t-\tau}\mathrm{d}\tau = 1 - t^2 + R^2/2\ , \tag{206}$$

where I used the following auxiliary integral (proof left as an exercise)

$$\mathrm{Pr}\int_{-1}^{1}\mathrm{d}y\ \frac{\sqrt{1-y^2}\ y}{x-y} = \pi\left(x^2-\frac{1}{2}\right)\qquad \text{for } x\in(-1,1)\ . \tag{207}$$

Clearly, $P_R(t)\geq 0$ over the full support $[-R,R]$ only if $R\leq R_\star = \sqrt{2}$. If $R>R_\star$, then $P_R(t)$ can be ≥ 0 only over a narrower interval $[-\sqrt{1+R^2/2},\sqrt{1+R^2/2}]$. Imposing $\sqrt{1+R^2/2} = R$ gives $R = R_\star = \sqrt{2}$, for which $P_{R_\star}(t) = 2-t^2$, and $n_{R_\star}^\star(t) = (1/\pi)\sqrt{2-t^2}$. Therefore, for the Gaussian case we have

$$n_R^\star(t) = \begin{cases} \frac{1-t^2+R^2/2}{\pi\sqrt{R^2-t^2}}\mathbb{1}_{-R\leq t\leq R} & \text{for } R<R_\star=\sqrt{2} \\ \frac{1}{\pi}\sqrt{R_\star^2-t^2}\mathbb{1}_{-R_\star\leq t\leq R_\star} & \text{for } R\geq R_\star = \sqrt{2}\ , \end{cases} \tag{208}$$

which is consistent with the physical picture that when the walls are not active ($R>R_\star$), the equilibrium density sticks to the unperturbed semicircular law. Mathematically, this abrupt change of shape of the equilibrium density – from a situation where the density diverges at the edges $\pm R$ of the support to one where the density vanishes as a square root at the edges $\pm R_\star$ of the support – is induced by the positivity constraint of the density over its entire support.

---

[18] This means the limit $\lim_{\epsilon\to 0}\left[\int^{x-\epsilon}F(x')\mathrm{d}x' + \int_{x+\epsilon}F(x')\mathrm{d}x'\right]$, if x is a singular point of $F(x)$.

To summarize, the cumulative distribution of the spectral radius for log-gases subject to an external potential satisfying **Assumption 1** reads

$$\mathrm{Prob}\left[\max_j |x_j| \leq R\right] = \frac{Z_N(R)}{Z_N(\infty)} \approx \exp\left[-\beta N^2 \underbrace{\left(\mathcal{E}[n^\star_R(x)] - \mathcal{E}[n^\star_{R_\star}(x)]\right)}_{F(R)}\right] \,, \tag{209}$$

where the mean-field energy functional is given by

$$\mathcal{E}[\sigma] = \int_{-R}^{R} \mathrm{d}x\ \sigma(x)V(x) - \frac{1}{2}\iint_{[-R,R]^2} \mathrm{d}x\mathrm{d}x'\sigma(x)\sigma(x')\log|x-x'| \,, \tag{210}$$

and its minimizer $n^\star_R(x)$ has the following general form

$$n^\star_R(t) = \begin{cases} \frac{P_R(t)}{\pi\sqrt{R^2-t^2}}\mathbb{1}_{-R\leq t\leq R} & \text{for } R < R_\star \text{ (pushed phase)} \\ \frac{1}{\pi}Q(t)\sqrt{R_\star^2 - t^2}\mathbb{1}_{-R_\star\leq t\leq R_\star} & \text{for } R \geq R_\star \text{ (pulled phase)} \,, \end{cases} \tag{211}$$

where

$$Q(t) = \lim_{R\to R_\star} \frac{P_R(t)}{R^2-t^2} \ . \tag{212}$$

The critical value $R_\star$ will be determined as the smallest positive solution of Eq. (226) below.

Inserting (208) into (210) and evaluating $F(R)$ from (209) provides the result derived by [58] (see Eq. (174)) for the Gaussian β-ensembles. This derivation is left as an exercise.

For a *general* potential $V(x)$, it seems difficult to be able to go much beyond this general summary: to compute $F(R)$ and evaluate the order of the phase transition as $R \to R_\star$, one would need to solve the integrals (210), which can only be done by specifying (on a case-by-case basis) the potential $V(x)$ at hand. Is this really the case, though?

In [30], we have actually managed to prove a general formula for the excess free energy (rate function) for r_2 in the form

$$\boxed{F(R) = \frac{1}{2}\int_{\min(R,R_\star)}^{R_\star} \frac{P_r^2(r)}{r}\mathrm{d}r} \,, \tag{213}$$

where $P_r(r)$ is the numerator of the equilibrium density in the pushed phase (see (211)), where both the parameter and the argument are set to the integration variable r.

The formula is based on the intriguing identity

$$-\log|x-y| = \log 2 + \sum_{n\geq 1}\frac{2}{n}T_n(x)T_n(y) \qquad |x|\leq 1, |y|\leq 1, x\neq y \,, \tag{214}$$

where T_n's are the Chebyshev polynomials of the first kind, defined by the relation

$$T_n(\cos\theta) = \cos(n\theta) \ . \tag{215}$$

These polynomials are orthogonal on $[-1,1]$ with respect to the "arcsine" measure

$$\int_{-1}^{1}\frac{T_n(x)T_m(x)}{\sqrt{1-x^2}}\mathrm{d}x = h_n\delta_{nm} \qquad \text{with } h_n = \begin{cases}\pi & n=m=0 \\ \frac{\pi}{2} & n=m\geq 1\end{cases} \ . \tag{216}$$

They also form a complete basis of $\mathcal{L}^2([-1,1])$. The first few polynomials are

$$T_0(x) = 1 \tag{217}$$

$$T_1(x) = x \tag{218}$$

$$T_2(x) = 2x^2 - 1 \,, \tag{219}$$

and in general

$$T_{n+1}(x) = 2xT_n(x) - T_{n-1}(x) \ . \tag{220}$$

The above identity was recently used and discussed in [133, 134] (the authors refer to some unpublished lecture notes by U. Haagerup).

I now proceed to proving it. Calling $X = \arccos x$ and $Y = \arccos y$, we first evaluate the auxiliary sum

$$S = \sum_{n\geq 1} \frac{\cos(nX)\cos(nY)}{n} \ . \tag{221}$$

Using the trigonometric identity

$$2\cos\alpha\cos\beta = \cos(\alpha-\beta) + \cos(\alpha+\beta) \ , \tag{222}$$

we have

$$\begin{aligned} S &= \frac{1}{2}\left[\sum_{n\geq 1}\frac{\cos(n(X-Y))}{n} + \sum_{n\geq 1}\frac{\cos(n(X+Y))}{n}\right] = \frac{1}{2}\mathrm{Re}\left[\sum_{n\geq 1}\frac{\exp(\mathrm{i}n(X-Y))}{n} + \sum_{n\geq 1}\frac{\exp(\mathrm{i}n(X+Y))}{n}\right] \\ &= -\frac{1}{2}\mathrm{Re}\left[\log(1-\mathrm{e}^{\mathrm{i}(X-Y)}) + \log(1-\mathrm{e}^{\mathrm{i}(X+Y)})\right] = -\frac{1}{4}\left[\log(2-2\cos(X-Y)) + \log(2-2\cos(X+Y))\right] \ , \end{aligned} \tag{223}$$

where we have used the Maclaurin expansion $\log(1-x) = -\sum_{n\geq 1} x^n/n$, the Euler formula $\mathrm{e}^{\mathrm{i}\theta} = \cos\theta + \mathrm{i}\sin\theta$ and $\mathrm{Re}\log z = \log|z|$. Therefore, all we need to compute is

$$\begin{aligned} \cos(X\pm Y) &= \cos\left(\arccos x \pm \arccos y\right) = \cos(\arccos x)\cos(\arccos y) \mp \sin(\arccos x)\sin(\arccos y) \\ &= xy \mp \sqrt{1-x^2}\sqrt{1-y^2} \ , \end{aligned} \tag{224}$$

using the standard trigonometric addition formula. After simplifications

$$S = -\frac{1}{4}\log[4(x-y)^2] = -\frac{1}{2}\left(\log 2 + \log|x-y|\right) \ . \tag{225}$$

Using now $\cos(nX) = T_n(\cos X) = T_n(x)$ (and similarly for Y) and substituting in (221), we establish the claim.

To prove the main formula (213), we first have to determine $R_\star$, the edge point of the constrained density in the pushed phase. This follows from a classical result in potential theory–see [131, 132]–which states that if the walls are not active (pulled phase) the density is supported on $[-R_\star, R_\star]$ with $R_\star$ solution of

$$\frac{1}{\pi}\int_{-R_\star}^{+R_\star} \frac{\tau V'(\tau)}{\sqrt{R_\star^2-\tau^2}}\mathrm{d}x = 1 \ . \tag{226}$$

While I will not prove this result in full generality, I can at least show that this condition follows easily from imposing that the equilibrium density in the pulled phase should vanish at the edge point, $n^\star_{R_\star}(R_\star) = 0$. This in turn would require the condition

$$P_{R_\star}(R_\star) = 0 \Rightarrow 1 - \mathrm{Pr}\int_{-R_\star}^{R_\star} \frac{1}{\pi}\frac{\sqrt{{R_\star}^2-\tau^2}V'(\tau)}{R_\star-\tau}\mathrm{d}\tau = 0 \tag{227}$$

from Eq. (205). Multiplying the integrand up and down by $R_\star + \tau$ yields

$$1 = R_\star \underbrace{\int_{-R_\star}^{R_\star} \frac{1}{\pi}\frac{V'(\tau)}{\sqrt{R_\star^2-\tau^2}}\mathrm{d}\tau}_{=0} + \int_{-R_\star}^{R_\star}\frac{1}{\pi}\frac{\tau V'(\tau)}{\sqrt{R_\star^2-\tau^2}}\mathrm{d}\tau \ , \tag{228}$$

where the first integral vanishes because the integrand is odd ($V(x)$ is even by **Assumption 1**). This quick derivation at least provides some rationale behind the condition (226). One could check as an exercise that for the Gaussian case, $V(x) = x^2/2$, the condition (226) yields back $R_\star = \sqrt{2}$.

In order to establish the main formula (213), we expand the potential V and the regular part of the equilibrium density into Chebyschev polynomials

$$V(Ru) = \sum_{n\geq 0} c_n(R)T_n(u) \ , \qquad P_R(Ru) = \sum_{n\geq 0} a_n(R)T_n(u) \ , \tag{229}$$

where

$$a_n(R) = \frac{1}{h_n}\int_{-1}^{1} \frac{P_R(Ru)T_n(u)}{\sqrt{1-u^2}}\mathrm{d}u \ , \qquad c_n(R) = \frac{1}{h_n}\int_{-1}^{1} \frac{V(Ru)T_n(u)}{\sqrt{1-u^2}}\mathrm{d}u \ . \tag{230}$$

A priori, the above expansions are in $\mathcal{L}^2([-1,1])$. In fact, $V \in C^3$ implies that $c_n(R) = \mathcal{O}(n^{-3})$ so that the series $\sum_{n\geq 0} c_n(R)T_n(u)$ and its derivative are pointwise convergent almost everywhere to V and V', respectively. We will see in the course of the proof that the absolute convergence of $\sum_n nc_n(R)$ implies the pointwise convergence of $\sum_n a_n(R)T_n(u)$, too. Note also that $c_n = 0$ if n is odd (the potential $V(x)$ is symmetric by **Assumption 1**). To proceed we use the following identity. Let $n \geq 0$ be an even integer. Then,

$$uT_n'(u) = nT_0(u) + nT_n(u) + 2n\left(T_2(u) + T_4(u) + \cdots + T_{n-2}(u)\right) \ . \tag{231}$$

We first express the condition (226) for the critical edge point $R_\star$ in terms of the c_n's. After the change of variable $x = R_\star u$, Eq. (226) becomes

$$1 = \frac{R_\star}{\pi}\int_{-1}^{1} uV'(R_\star u)\frac{\mathrm{d}u}{\sqrt{1-u^2}} = \frac{1}{\pi}\int_{-1}^{1}\sum_{n\geq 0} c_n(R_\star)uT_n'(u)\frac{\mathrm{d}u}{\sqrt{1-u^2}} = \sum_{n\geq 0} nc_n(R_\star) \ , \tag{232}$$

where we used (231) and the orthogonality relation (216). Note that $nc_n(R_\star) = \mathcal{O}(n^{-2})$ and hence the series is absolutely convergent.

We now recall the Euler-Lagrange equation (197) in the pushed phase

$$V(x) - \int_{-R}^{R}\mathrm{d}x' \ n_R^\star(x')\log|x-x'| + \mu_R = 0 \ , \tag{233}$$

as well as the general expression for the equilibrium density (211)

$$n_R^\star(x) = \frac{P_R(x)}{\pi\sqrt{R^2-x^2}} \ . \tag{234}$$

Setting $x = Ru$ and $x' = Ru'$, we can apply the expansion (214) of the logarithmic interaction term, as well as the expansions (229) for the potential and the numerator $P_R(x)$ to obtain

$$-\log R + R\int_{-1}^{1}\mathrm{d}u' \ \left[\log 2 + \sum_{n\geq 1}\frac{2}{n}T_n(u)T_n(u')\right]\frac{1}{\pi R\sqrt{1-u'^2}}\sum_{m\geq 0} a_m(R)T_m(u') + \sum_{n\geq 0} c_n(R)T_n(u) + \mu_R = 0 \ . \tag{235}$$

This leads to

$$-\log\frac{R}{2} + \frac{1}{\pi}\sum_{m,n}\frac{2}{n}a_m(R)T_n(u)\underbrace{\int_{-1}^{1}\frac{T_n(u')T_m(u')}{\sqrt{1-u'^2}}\mathrm{d}u'}_{h_n\delta_{nm}} + c_0(R) + \sum_{n\geq 1} c_n(R)T_n(u) + \mu_R = 0 \tag{236}$$

leading eventually to

$$-\log\frac{R}{2} + c_0(R) + \sum_{n\geq 1}\left(\frac{1}{n}a_n(R) + c_n(R)\right)T_n(u) = -\mu_R \quad \text{if } |u| \leq 1 \ . \tag{237}$$

To ensure that the l.h.s. is indeed equal to a R-dependent constant, we need to kill any u-dependence on the l.h.s. . This provides the condition

$$\frac{1}{n}a_n(R) + c_n(R) = 0 \qquad \forall n \geq 1 \tag{238}$$

between the coefficients of the expansion of the external potential and the regular term of the constrained density. As a byproduct, we also obtain an explicit formula for the chemical potential

$$\mu_R = \log\frac{R}{2} - c_0(R) = \log\frac{R}{2} - \int_{-R}^{R}\frac{V(x)}{\pi\sqrt{R^2-x^2}}\mathrm{d}x \ . \tag{239}$$

Combining (238) with (229) and using $a_0(R) = 1$ (which follows from density normalization) shows that

$$P_R(Ru) = 1 - \sum_{n\geq 1} nc_n(R) T_n(u) \ . \tag{240}$$

The sequence $nc_n(R)$ is $\mathcal{O}(n^{-2})$ and hence the series is pointwise convergent almost everywhere.

Now, we focus on the excess free energy for the distribution of $r_2 = \max_j |x_j|$ in case of a general confining potential satisfying **Assumption 1** (see (209))

$$\begin{aligned} F(R) = \mathcal{E}[n_R^\star(x)] - \mathcal{E}[n_{R_\star}^\star(x)] = \\ \int_{-R}^{R} \mathrm{d}x \ n_R^\star(x) V(x) - \frac{1}{2} \iint_{[-R,R]^2} \mathrm{d}x\mathrm{d}x' n_R^\star(x) n_R^\star(x') \log|x-x'| - \mathcal{C}(R_\star) \ , \end{aligned} \tag{241}$$

where

$$\mathcal{C}(R_\star) = \int_{-R_\star}^{R_\star} \mathrm{d}x \ n_{R_\star}^\star(x) V(x) - \frac{1}{2} \iint_{[-R_\star,R_\star]^2} \mathrm{d}x\mathrm{d}x' n_{R_\star}^\star(x) n_{R_\star}^\star(x') \log|x-x'| \ . \tag{242}$$

The relation (241) can be significantly simplified by appealing to the Euler-Lagrange equation (233). Multiplying Eq. (233) by $n_R^\star(x)$ and integrating over x, we get the following identity for the double integral appearing in (241)

$$\iint_{[-R,R]^2} \mathrm{d}x\mathrm{d}x' n_R^\star(x) n_R^\star(x') \log|x-x'| = \int_{-R}^{R} \mathrm{d}x \ n_R^\star(x) V(x) + \mu_R \ , \tag{243}$$

leading to

$$F(R) = \frac{1}{2}\left[\int_{-R}^{R} \mathrm{d}x \ n_R^\star(x) V(x) - \mu_R\right] - \mathcal{C}(R_\star) \ . \tag{244}$$

Expanding (244) using (229)

$$\begin{aligned} F(R) &= \frac{1}{2}\left(-\mu_R + \int_{-1}^{1} V(Ru) \frac{P_R(Ru)}{\pi\sqrt{1-u^2}} \mathrm{d}u\right) - \mathcal{C}(R_\star) \\ &= \frac{1}{2}\left(-\mu_R + \sum_{n,m\geq 0} c_n(R) a_m(R) \int_{-1}^{1} \frac{T_n(u)T_m(u)}{\pi\sqrt{1-u^2}} \mathrm{d}u\right) - \mathcal{C}(R_\star) \\ &= \frac{1}{2}\left(-\mu_R + c_0(R)a_0(R) + \frac{1}{2}\sum_{n\geq 1} c_n(R) a_n(R)\right) - \mathcal{C}(R_\star) \\ &= \frac{1}{2}\left(-\log\frac{R}{2} + 2c_0(R) - \sum_{n\geq 1} \frac{nc_n^2(R)}{2}\right) - \mathcal{C}(R_\star) \ . \end{aligned} \tag{245}$$

I used the orthogonality condition, the fact that $a_0(R) = 1$, the equation (239) for the chemical potential, and the relation (238) between the coefficients $a_n(R)$ and $c_n(R)$ of the expansion.

Differentiating Eq. (245) w.r.t. R

$$F'(R) = -\frac{1}{2R}\left(1 - 2Rc_0'(R) + R\sum_{n\geq 1} nc_n(R) c_n'(R)\right) \ . \tag{246}$$

To establish the main formula (213), it is sufficient to prove that the above expression (246) is equal to $-P_R(R)^2/(2R)$. First, notice from (240) that $P_R(R)$ is

$$P_R(R) = \sum_{n\geq 0} a_n(R) T_n(1) = \sum_{n\geq 0} a_n(R) = 1 - \sum_{n\geq 1} nc_n(R) \ ,$$

so that

$$-\frac{P_R(R)^2}{2R} = -\frac{1}{2R}\left(1-\sum_{n\geq 1} nc_n(R)\right)^2 . \tag{247}$$

Comparing with (246), the identity to show to complete the proof is

$$1-2Rc_0'(R)+R\sum_{n\geq 1} nc_n(R)c_n'(R) \stackrel{?}{=} \left(1-\sum_{n\geq 1} nc_n(R)\right)^2 . \tag{248}$$

We need an identity to express the derivatives $c_n'(R)$ of the coefficient $c_n(R)$, which appear in (248). We may use $u\partial V(Ru)/\partial u = R\partial V(Ru)/\partial R$, together with $V(Ru)=\sum_{n\geq 0} c_n(R)T_n(u)$ from (229) to get

$$\sum_{m\geq 1} c_m(R)uT_m'(u) = \sum_{n\geq 0} Rc_n'(R)T_n(u) . \tag{249}$$

We can now use the identity (231) to get

$$\sum_{m\geq 1} c_m(R)\sum_{\ell=0}^{m} d_\ell(m)T_\ell(u) = \sum_{n\geq 0} Rc_n'(R)T_n(u) , \tag{250}$$

where the coefficients $d_0(m)=d_m(m)=m$, $d_\ell(m)=2m$ for ℓ even between 2 and $m-2$, and 0 otherwise. We now need to match coefficients corresponding to the same polynomial on both sides. To do so, we use the identity

$$\sum_{m\geq 1}\sum_{\ell=0}^{m} f(m,\ell) = \sum_{n\geq 0}\sum_{m\geq n}^{m} f(m,n) - f(0,0) \tag{251}$$

and then match the coefficients of $T_n(u)$ on both sides of (250). Take for instance $n=0$. The coefficient of $T_0(u)$ on the r.h.s. is $Rc_0'(R)$, whereas on the l.h.s. we have (taking into account that $f(0,0)=0$ since $d_0(0)=0$)

$$\sum_{m\geq n=0} c_m(R)d_{n=0}(m) = \sum_{m\geq n=0} c_m(R)m = \sum_{m\geq 1} c_m(R)m . \tag{252}$$

In summary, we get

$$c_n'(R) = \begin{cases} \displaystyle\sum_{m\geq 1}\frac{mc_m(R)}{R} & \text{if } n=0 \\ \displaystyle\sum_{m\geq n}\frac{2mc_m(R)}{R} - \frac{nc_n(R)}{R} & \text{if } n>0 . \end{cases} \tag{253}$$

Therefore we find for the l.h.s. of (248)

$$1-2Rc_0'(R)+R\sum_{n\geq 1} nc_n(R)c_n'(R) \tag{254}$$

$$= 1-2\sum_{m\geq 1} mc_m(R) + \sum_{n\geq 1} nc_n(R)\left(\sum_{m\geq n} 2mc_m(R) - nc_n(R)\right) \tag{255}$$

$$= 1-2\sum_{m\geq 1} mc_m(R) + \sum_{m,n\geq 1} nc_n(R)mc_m(R) \tag{256}$$

$$= \left(1-\sum_{n\geq 1} nc_n(R)\right)^2 , \tag{257}$$

which essentially concludes the proof of the integral formula (213) for $F(R)$, where we have used that

$$\sum_{n\geq 1} f(n) \sum_{1\leq m\leq n} f(m) = \sum_{n\geq 1} f(n) \sum_{m\geq n} f(m) \ . \tag{258}$$

We now proceed to prove that $F(R)$ has always a jump in the third derivative at $R = R_\star$. First, note that $F(R)$ is identically zero for $R \geq R_\star$, while $F(R) \geq 0$ for $R \leq R_\star$. From (213) and the fact that $P_{R_\star}(R_\star) = 0$, one sees that

$$\lim_{R\uparrow R_\star} F(R) = \frac{1}{2}\int_{R_\star}^{R_\star} \frac{P_r(r)^2}{r} \mathrm{d}r = 0 \ , \tag{259}$$

$$\lim_{R\uparrow R_\star} F'(R) = -\frac{1}{2}\frac{P_{R_\star}(R_\star)^2}{R_\star} = 0 \ , \tag{260}$$

$$\lim_{R\uparrow R_\star} F''(R) = -\frac{2P_{R_\star}(R_\star)P'_{R_\star}(R_\star)R_\star - P_{R_\star}(R_\star)^2}{2R_\star^2} = 0 \ . \tag{261}$$

On the other hand,

$$\lim_{R\uparrow R_\star} F'''(R) = -\frac{P'_{R_\star}(R_\star)^2}{R_\star} < 0 \ . \tag{262}$$

Indeed, by **Assumption 1** on the potential $V(x)$, it is possible to check that $P'_{R_\star}(R_\star) < 0$ strictly. Computing further derivative allows us to understand what conditions must happen for the potential to get an even weaker phase transition. Our proof valid for one-cut and off-critical potentials fully and rigorously confirms the Majumdar-Schehr criterion for the existence of a third-order phase transition.

B. Appendix: Derivation of the entropic term in Eq. (194)

Consider the term in Eq. (193)

$$\Psi[n_R(x)] = \int_{-R}^{R}\cdots\int_{-R}^{R} \mathrm{d}x_1\cdots \mathrm{d}x_N \delta\left[n_R(x) - \frac{1}{N}\sum_i \delta_{x,x_i}\right] \ . \tag{263}$$

Introducing a Fourier representation of the functional delta (the functional analog to Eq. (109)), we can write (omitting overall constants)

$$\begin{aligned}\Psi[n_R(x)] &\propto \int \mathcal{D}[\hat{n}_R(x)]\mathrm{e}^{\mathrm{i}N\int \mathrm{d}x\ \hat{n}_R(x)n_R(x)} \int_{-R}^{R}\cdots\int_{-R}^{R} \mathrm{d}x_1\cdots \mathrm{d}x_N\ \mathrm{e}^{-\mathrm{i}\int \mathrm{d}x\ \hat{n}_R(x)\sum_i \delta_{x,x_i}} \\ &\propto \int \mathcal{D}[\hat{n}_R(x)]\mathrm{e}^{\mathrm{i}N\int \mathrm{d}x\ \hat{n}_R(x)n_R(x)} \left[\int_{-R}^{R} \mathrm{d}z\ \mathrm{e}^{-\mathrm{i}\int \mathrm{d}x\ \hat{n}_R(x)\delta_{x,z}}\right]^N \ ,\end{aligned} \tag{264}$$

where in the last step one uses that the multiple $\{x_i\}$ integral factorizes into N identical copies of the same integral. Using now the delta to kill the z-integral, and re-casting the integral in a more convenient form, we get

$$\Psi[n_R(x)] \propto \int \mathcal{D}[\hat{n}_R(x)]\mathrm{e}^{N\mathcal{S}[\hat{n}_R(x),n_R(x)]} \approx \mathrm{e}^{N\mathcal{S}[\hat{n}_R^\star(x),n_R(x)]} \tag{265}$$

for large N, where the action reads

$$\mathcal{S}[\hat{n}_R(x), n_R(x)] = \mathrm{i}\int \mathrm{d}x\ \hat{n}_R(x)n_R(x) + \log\int_{-R}^{R} \mathrm{d}z\ \mathrm{e}^{-\mathrm{i}\hat{n}_R(z)} \ . \tag{266}$$

The functional integral (265) can then be evaluated by a saddle-point method for large N. The saddle-point equation reads

$$\left.\frac{\delta\mathcal{S}}{\delta\hat{n}_R(x)}\right|_{\hat{n}_R=\hat{n}_R^\star} = 0 \Rightarrow \mathrm{i}n_R(x) - \mathrm{i}\frac{\mathrm{e}^{-\mathrm{i}\hat{n}_R^\star(x)}}{\int_{-R}^{R}\mathrm{d}z\ \mathrm{e}^{-\mathrm{i}\hat{n}_R^\star(z)}} = 0 \ . \tag{267}$$

We see by inspection that $\mathrm{e}^{-\mathrm{i}\hat{n}_R^\star(x)} = n_R(x)$ is a solution of the above equation, since $\int_{-R}^{R} \mathrm{d}z\, \mathrm{e}^{-\mathrm{i}\hat{n}_R^\star(z)} = \int_{-R}^{R} \mathrm{d}z\, n_R(z) = 1$ by normalization. Therefore $\mathrm{i}\hat{n}_R^\star(x) = -\log \hat{n}_R^\star(x)$, which gives the action at the saddle point

$$\mathcal{S}[\hat{n}_R^\star(x), n_R(x)] = -\int \mathrm{d}x\; n_R(x) \log n_R(x) \;, \tag{268}$$

which can be inserted back into (265) to give eventually Eq. (194).

---

[1] Touchette, H. (2009). *The large deviation approach to statistical mechanics.* Physics Reports, **478(1-3)**, 1-69.
[2] Alastuey, A., & Jancovici, B. (1981). *On the classical two-dimensional one-component Coulomb plasma.* Journal de Physique, **42(1)**, 1-12.
[3] Cornu, F., & Jancovici, B. (1988). *Two-dimensional Coulomb systems: a larger class of solvable models.* Europhysics Letters, **5(2)**, 125.
[4] Dyson, F. J. (1962). *Statistical Theory of the Energy Levels of Complex Systems*, J. Math. Phys., **3**, 140; **3**, 157; **3**, 166; **3**, 1191; **3**, 1199.
[5] Forrester, P. (1998). *Exact results for two-dimensional Coulomb systems.* Physics Reports, **301(1-3)**, 235-270.
[6] Jancovici, B. (1981). *Exact results for the two-dimensional one-component plasma.* Physical Review Letters, **46(6)**, 386.
[7] Johannesen, S., & Merlini, D. (1983). *On the thermodynamics of the two-dimensional jellium.* Journal of Physics A: Mathematical and General, **16(7)**, 1449.
[8] Sari, R. R., Merlini, D., & Calinon, R. (1976). *On the ground state of the one-component classical plasma.* Journal of Physics A: Mathematical and General, **9(9)**, 1539.
[9] Zabrodin, A., & Wiegmann, P. (2006). *Large-N expansion for the 2D Dyson gas.* Journal of Physics A: Mathematical and General, **39(28)**, 8933.
[10] Sandier, E., & Serfaty, S. (2012). *From the Ginzburg-Landau model to vortex lattice problems.* Communications in Mathematical Physics, **313**, 635-743.
[11] Correggi, M., & Yngvason, J. (2008). *Energy and vorticity in fast rotating Bose–Einstein condensates.* Journal of Physics A: Mathematical and Theoretical, **41(44)**, 445002.
[12] Correggi, M., Pinsker, F., Rougerie, N., & Yngvason, J. (2012). *Critical rotational speeds for superfluids in homogeneous traps.* Journal of Mathematical Physics, **53(9)**.
[13] Rougerie, N., Serfaty, S., & Yngvason, J. (2014). *Quantum Hall phases and plasma analogy in rotating trapped Bose gases.* Journal of Statistical Physics, **154**, 2-50.
[14] Aftalion, A. (2007). *Vortices in Bose-Einstein Condensates* (Vol. **67**). Springer Science & Business Media.
[15] Serfaty, S. *Coulomb Gases and Ginzburg-Landau Vortices*, Courant Institute of Mathematical Sciences, New York, NY (2014); *Ginzburg-Landau Vortices, Coulomb Gases, and Renormalized Energies*, J. Stat. Phys. **154**, 660-680 (2014).
[16] Laughlin, R. B. (1983). *Anomalous quantum Hall effect: an incompressible quantum fluid with fractionally charged excitations.* Physical Review Letters, **50(18)**, 1395.
[17] Can, T., Forrester, P. J., Téllez, G., & Wiegmann, P. *Singular behavior at the edge of Laughlin states*, Phys. Rev. B **89**, 235137 (2014); *Exact and asymptotic features of the edge density profile for the one component plasma in two dimensions*, J. Stat. Phys. **158**, 1147-1180 (2015).
[18] Zabrodin, A. *Random matrices and Laplacian growth*, a contribution to Akemann, G., Baik, J., & Di Francesco, P. (2011). *The Oxford handbook of random matrix theory.* Oxford University Press.
[19] Bordenave, C. & Chafaï, C. *Around the circular law*, Probability Surveys **9**, 1-89 (2012).
[20] Forrester, P. J. (2010). *Log-gases and random matrices (LMS-34).* Princeton University Press.
[21] Khoruzhenko, B. & Sommers, H.-J. *Non-Hermitian ensembles*, a contribution to Akemann, G., Baik, J., & Di Francesco, P. (2011). *The Oxford handbook of random matrix theory.* Oxford University Press.
[22] Zabrodin, A. (2006). *Matrix models and growth processes: from viscous flows to the quantum Hall effect.* In Applications of Random Matrices in Physics (pp. 261-318). Springer Netherlands.
[23] Ginibre, J. (1965). *Statistical ensembles of complex, quaternion, and real matrices.* Journal of Mathematical Physics, **6(3)**, 440-449.
[24] Hsu, P. L. (1939). *On the distribution of roots of certain determinantal equations.* Annals of Eugenics, **9(3)**, 250-258.
[25] Porter, C. E., & Rosenzweig, N. (1960). *Statistical properties of atomic and nuclear spectra.* Ann. Acad. Sci. Fennicae, Serie A VI Physica 6, 44 (1960), reprinted in Porter, C.E. *Statistical Theories of Spectra: Fluctuations* (Academic Press, New York, 1965).
[26] Livan, G., Novaes, M., & Vivo, P. (2018). *Introduction to random matrices theory and practice.* SpringerBriefs in Mathematical Physics, online at [`https://arxiv.org/abs/1712.07903`].
[27] Majumdar, S. N., & Vergassola, M. (2009). *Large deviations of the maximum eigenvalue for Wishart and Gaussian random matrices.* Physical Review Letters, **102(6)**, 060601.
[28] Majumdar, S. N., & Schehr, G. (2014). *Top eigenvalue of a random matrix: large deviations and third order phase transition.* Journal of Statistical Mechanics: Theory and Experiment, **2014(1)**, P01012.
[29] Fyodorov, Y. V., & Le Doussal, P. (2014). *Topology trivialization and large deviations for the minimum in the simplest random optimization.* Journal of Statistical Physics, **154(1)**, 466-490.

[30] Cunden, F. D., Facchi, P., Ligabò, M., & Vivo, P. (2019). *Third-order phase transition: random matrices and screened Coulomb gas with hard walls.* Journal of Statistical Physics, **175(6)**, 1262-1297.

[31] Edelman, A., & Persson, P. O. (2005). *Numerical methods for eigenvalue distributions of random matrices.* Preprint arXiv [math-ph/0501068].

[32] Tracy, C. A., & Widom, H. (1994). *Level-spacing distributions and the Airy kernel.* Communications in Mathematical Physics, **159**, 151-174.

[33] Tracy, C. A., & Widom, H. (1996). *On orthogonal and symplectic matrix ensembles.* Communications in Mathematical Physics, **177**, 727-754.

[34] Edelman, A., & Sutton, B. D. (2007). *From random matrices to stochastic operators.* Journal of Statistical Physics, **127**, 1121-1165.

[35] Ramirez, J., Rider, B., & Virág, B. (2011). *Beta ensembles, stochastic Airy spectrum, and a diffusion.* Journal of the American Mathematical Society, **24(4)**, 919-944.

[36] Johnstone, I. M. (2001). *On the distribution of the largest eigenvalue in principal components analysis.* The Annals of Statistics, **29(2)**, 295-327.

[37] Soshnikov, A. (2002). *A note on universality of the distribution of the largest eigenvalues in certain sample covariance matrices.* Journal of Statistical Physics, **108**, 1033-1056.

[38] Johansson, K. (2000). *Shape fluctuations and random matrices.* Communications in Mathematical Physics, **209**, 437-476.

[39] Majumdar, S. N., Les Houches lecture notes on *Complex Systems* (2006), ed. by J.-P. Bouchaud, M. Mézard and J. Dalibard, online at [`https://arxiv.org/abs/cond-mat/0701193`].

[40] Baik, J., Deift, P., & Johansson, K. (1999). *On the distribution of the length of the longest increasing subsequence of random permutations.* Journal of the American Mathematical Society, **12(4)**, 1119-1178.

[41] Baik, J., & Rains, E. M. (2000). *Limiting distributions for a polynuclear growth model with external sources. Journal of Statistical Physics*, **100**, 523-541.

[42] M. Prähofer, H. Spohn, Phys. Rev. Lett. **84**, 4882 (2000); Gravner, J., Tracy, C. A., Widom, H., J. Stat. Phys. **102**, 1085 (2001); Majumdar,S. N., Nechaev, S., Phys. Rev. E **69**, 011103 (2004); Imamura, T. , Sasamoto, T. Nucl. Phys. B **699**, 503 (2004).

[43] Sasamoto, T., & Spohn, H. (2010). *One-dimensional Kardar-Parisi-Zhang equation: an exact solution and its universality.* Physical Review Letters, 1**04(23)**, 230602.

[44] Calabrese, P., Le Doussal, P., & Rosso, A. (2010). *Free-energy distribution of the directed polymer at high temperature.* Europhysics Letters, **90(2)**, 20002.

[45] Dotsenko, V. (2010). *Bethe ansatz derivation of the Tracy-Widom distribution for one-dimensional directed polymers.* Europhysics Letters, **90(2)**, 20003.

[46] Amir, G., Corwin, I., & Quastel, J. (2011). *Probability distribution of the free energy of the continuum directed random polymer in $1+1$ dimensions.* Communications on Pure and Applied Mathematics, **64(4)**, 466-537.

[47] Majumdar, S. N., & Nechaev, S. (2005). *Exact asymptotic results for the Bernoulli matching model of sequence alignment.* Physical Review E - Statistical, Nonlinear, and Soft Matter Physics, **72(2)**, 020901.

[48] M. G. Vavilov, P. W. Brouwer, V. Ambegaokar, C. W. J. Beenakker, Phys. Rev. Lett. **86**, 874 (2001); A. Lamacraft, B. D. Simons, Phys. Rev. B **64**, 014514 (2001); P. M. Ostrovsky, M. A. Skvortsov, M. V. Feigel'man, Phys. Rev. Lett. **87**, 027002 (2001); J. S. Meyer, B. D. Simons, Phys. Rev. B **64**, 134516 (2001); A. Silva, L. B. Ioffe, Phys. Rev. B **71**, 104502 (2005).

[49] Liechty, K. (2012). *Nonintersecting Brownian motions on the half-line and discrete Gaussian orthogonal polynomials.* Journal of Statistical Physics, **147**, 582-622.

[50] Forrester, P. J., Majumdar, S. N., & Schehr, G. (2011). *Non-intersecting Brownian walkers and Yang–Mills theory on the sphere.* Nuclear Physics B, **844(3)**, 500-526.

[51] Nadal, C., & Majumdar, S. N. (2009). *Nonintersecting Brownian interfaces and Wishart random matrices.* Physical Review E - Statistical, Nonlinear, and Soft Matter Physics, **79(6)**, 061117.

[52] Biroli, G., Bouchaud, J. P., & Potters, M. (2007). *On the top eigenvalue of heavy-tailed random matrices.* Europhysics Letters, **78(1)**, 10001.

[53] K . A. Takeuchi, M. Sano, Phys. Rev. Lett. **104**, 230601 (2010); K . A. Takeuchi, M. Sano, T. Sasamoto, H. Spohn, Sci. Rep. (Nature) **1**, 34 (2011); K . A. Takeuchi, M. Sano, J. Stat. Phys. **147**, 853 (2012).

[54] Fridman, M., Pugatch, R., Nixon, M., Friesem, A. A., & Davidson, N. (2012). *Measuring maximal eigenvalue distribution of Wishart random matrices with coupled lasers.* Physical Review E - Statistical, Nonlinear, and Soft Matter Physics, **85(2)**, 020101.

[55] Bowick, M. J., & Brézin, É. (1991). *Universal scaling of the tail of the density of eigenvalues in random matrix models.* Physics Letters B, **268(1)**, 21-28.

[56] Forrester, P. J. (1993). *The spectrum edge of random matrix ensembles.* Nuclear Physics B, **402(3)**, 709-728.

[57] Dean, D. S., & Majumdar, S. N. (2006). *Large deviations of extreme eigenvalues of random matrices.* Physical Review Letters, **97(16)**, 160201.

[58] Dean, D. S., & Majumdar, S. N. (2008). *Extreme value statistics of eigenvalues of Gaussian random matrices.* Physical Review E -Statistical, Nonlinear, and Soft Matter Physics, **77(4)**, 041108.

[59] Ben Arous, G., Dembo, A., & Guionnet, A. (2001). *Aging of spherical spin glasses.* Probability theory and related fields, **120**, 1-67.

[60] Forrester, P. J. (2012). *Spectral density asymptotics for Gaussian and Laguerre β-ensembles in the exponentially small region.* Journal of Physics A: Mathematical and Theoretical, **45(7)**, 075206.

[61] Fyodorov, Y. V. (2004). *Complexity of Random Energy Landscapes, Glass Transition, and Absolute Value of the Spectral Determinant of Random Matrices.* Physical Review Letters, **92(24)**, 240601.; Erratum Phys. Rev. Lett. **93**, 149901.

[62] Vivo, P., Majumdar, S. N., & Bohigas, O. (2007). *Large deviations of the maximum eigenvalue in Wishart random matrices.* Journal of Physics A: Mathematical and Theoretical, **40(16)**, 4317.

[63] See `https://functions.wolfram.com/HypergeometricFunctions/Hypergeometric3F2/03/08/06/01/02/08/0004/`

[64] Nadal, C., & Majumdar, S. N. (2011). *A simple derivation of the Tracy–Widom distribution of the maximal eigenvalue of a Gaussian unitary random matrix.* Journal of Statistical Mechanics: Theory and Experiment, **2011(04)**, P04001.

[65] Gross, D. J., & Matytsin, A. (1994). *Instanton induced large N phase transitions in two-and four-dimensional QCD.* Nuclear Physics B, **429(1)**, 50-74.

[66] Borot, G., & Nadal, C. (2012). *Purity distribution for generalized random Bures mixed states.* Journal of Physics A: Mathematical and Theoretical, **45(7)**, 075209. *Right tail asymptotic expansion of Tracy–Widom beta laws.* Random Matrices: Theory and Applications, **1(03)**, 1250006.

[67] Akemann, G., & Atkin, M. R. (2012). *Higher order analogues of Tracy–Widom distributions via the Lax method.* Journal of Physics A: Mathematical and Theoretical, **46(1)**, 015202.

[68] Atkin, M. R., & Zohren, S. (2014). *Instantons and extreme value statistics of random matrices.* Journal of High Energy Physics, **2014(4)**, 1-31.

[69] Guionnet, A., & Husson, J. (2018). *Large deviations for the largest eigenvalue of Rademacher matrices.* Preprint [arXiv:1810.01188]

[70] Augeri, F. & Basak, A. (2023). *Large deviations of the largest eigenvalue of supercritical sparse Wigner matrices.* Preprint [arXiv:2304.13364]

[71] Biroli, G., & Guionnet, A. (2020). *Large deviations for the largest eigenvalues and eigenvectors of spiked Gaussian random matrices.* Electronic Communications in Probability, **25** article n. 70, 1–13.

[72] Mergny, P., & Potters, M. (2022). *Right large deviation principle for the top eigenvalue of the sum or product of invariant random matrices.* Journal of Statistical Mechanics: Theory and Experiment, **063301**.

[73] Ganguly, S., & Nam, K. (2022). *Large deviations for the largest eigenvalue of Gaussian networks with constant average degree.* Probability Theory and Related Fields, **184**, 613–679.

[74] Bordenave, C., & Caputo, P. (2014). *A large deviation principle for Wigner matrices without Gaussian tails.* Annals of Probability, **42(6)**, 2454-2496.

[75] Maida, M. (2007). *Large deviations for the largest eigenvalue of rank one deformations of Gaussian ensembles.* Electronic Journal of Probability, **12**, 1131-1150.

[76] Benaych-Georges, F., Guionnet, A. & Maida, M. (2012). *Large deviations of the extreme eigenvalues of random deformations of matrices.* Probability Theory and Related Fields **154**, 703–751.

[77] Maillard, A. (2021). *Large deviations of extreme eigenvalues of generalized sample covariance matrices.* Europhysics Letters, **133(2)**, 20005.

[78] Dumitriu, I., & Edelman, A. (2002). *Matrix models for beta ensembles.* Journal of Mathematical Physics **43**, 5830 (2002).

[79] Trefethen, L. N., & Bau, D. (2022). *Numerical linear algebra.* Society for Industrial and Applied Mathematics.

[80] Lacroix-A-Chez-Toine, B., Grabsch, A., Majumdar, S. N., & Schehr, G. (2018). *Extremes of* 2*d Coulomb gas: universal intermediate deviation regime.* Journal of Statistical Mechanics: Theory and Experiment, **2018(1)**, 013203.

[81] Rider, B. (2003). *A limit theorem at the edge of a non-Hermitian random matrix ensemble.* Journal of Physics A: Mathematical and General, **36(12)**, 3401.

[82] Cunden, F. D., Mezzadri, F., & Vivo, P. (2016). *Large deviations of radial statistics in the two-dimensional one-component plasma.* Journal of Statistical Physics, **164**, 1062-1081.

[83] Chafaï, D., & Péché, S. (2014). *A Note on the Second Order universality at the Edge of Coulomb Gases on the Plane*, Journal of Statistical Physics, **156**, 368-383.

[84] Vivo, P. (2015). *Large deviations of the maximum of independent and identically distributed random variables.* European Journal of Physics, **36(5)**, 055037.

[85] Kostlan, E. (1992). *On the spectra of Gaussian matrices.* Linear Algebra and its Applications, **162**, 385-388.

[86] Allez, R., Touboul, J., & Wainrib, G. (2014). *Index distribution of the Ginibre ensemble.* Journal of Physics A: Mathematical and Theoretical, **47(4)**, 042001.

[87] Cunden, F. D., Maltsev, A., & Mezzadri, F. (2015). *Fluctuations in the two-dimensional one-component plasma and associated fourth-order phase transition.* Physical Review E, **91(6)**, 060105.

[88] Jancovici, B., Lebowitz, J. L., & Manificat, G. (1993). *Large charge fluctuations in classical Coulomb systems.* Journal of Statistical Physics, **72**, 773-787.

[89] Lacroix-A-Chez-Toine, B., Monroy Garzón, J. A. , Hidalgo Calva, C. S., Pérez Castillo, I., Kundu, A., Majumdar, S. N.,& Schehr, G. (2019). *Intermediate deviation regime for the full eigenvalue statistics in the complex Ginibre ensemble.* Physical Review E, **100(1)**, 012137.

[90] Chafaï, D. & Péché, S. (2014). *A note on the second order universality at the edge of Coulomb gases on the plane.* Journal of Statistical Physics, **156**, 368-383.

[91] Ebrahimi, R., & Zohren, S. (2018). *On the extreme value statistics of normal random matrices and 2D Coulomb gases: universality and finite N corrections.* Journal of Statistical Mechanics: Theory and Experiment, **2018(3)**, 033301.

[92] Cunden, F. D., Facchi, P., Ligabò, M., & Vivo, P. (2017). *Universality of the third-order phase transition in the constrained Coulomb gas.* Journal of Statistical Mechanics: Theory and Experiment, **2017(5)**, 053303.

[93] Castellani, T., & Cavagna, A. (2005). *Spin-glass theory for pedestrians.* Journal of Statistical Mechanics: Theory and Experiment, **2005(05)**, P05012.
[94] Zamponi, F. (2010). *Mean field theory of spin glasses.* Preprint arXiv:1008.4844.
[95] Talagrand, M. (2010). *Mean field models for spin glasses: Volume I: Basic examples* (Vol. **54**). Springer Science & Business Media.
[96] Bovier, A. (2006). *Statistical mechanics of disordered systems: a mathematical perspective* (Vol. **18**). Cambridge University Press.
[97] Panchenko, D. (2013). *The Sherrington-Kirkpatrick model.* Springer Science & Business Media.
[98] Parisi, G., Urbani, P., & Zamponi, F. (2020). *Theory of simple glasses: exact solutions in infinite dimensions.* Cambridge University Press. .
[99] Ingham, A. E. (1933). *An integral which occurs in statistics.* In Mathematical Proceedings of the Cambridge Philosophical Society (Vol. **29**, No. 2, pp. 271-276). Cambridge University Press.
[100] Siegel, C. L. (1935). *Über die analytische Theorie der quadratischen Formen.* Annals of Mathematics, **36(3)**, 527-606.
[101] Fyodorov, Y. V. (2002). *Negative moments of characteristic polynomials of random matrices: Ingham–Siegel integral as an alternative to Hubbard–Stratonovich transformation.* Nuclear Physics B, **621(3)**, 643-674.
[102] Prussing, J. E. (1986). *The principal minor test for semidefinite matrices.* Journal of Guidance, Control, and Dynamics, **9(1)**, 121-122.
[103] Dean, D. S., Le Doussal, P., Majumdar, S. N., & Schehr, G. (2017). *Statistics of the maximal distance and momentum in a trapped Fermi gas at low temperature.* Journal of Statistical Mechanics: Theory and Experiment, **2017(6)**, 063301.
[104] Edelman, A., & La Croix, M. (2015). *The singular values of the GUE (less is more).* Random Matrices: Theory and Applications, **4(04)**, 1550021.
[105] Cunden, F. D., Facchi, P., & Vivo, P. (2016). *A shortcut through the Coulomb gas method for spectral linear statistics on random matrices.* Journal of Physics A: Mathematical and Theoretical, **49(13)**, 135202.
[106] Barranco, A., & Russo, J. G. (2014). *Large N phase transitions in supersymmetric Chern-Simons theory with massive matter.* Journal of High Energy Physics, **2014(3)**, 1-15.
[107] Gross, D. J., & Witten, E. (1980). *Possible third-order phase transition in the large-N lattice gauge theory.* Physical Review D, **21(2)**, 446.
[108] Santilli, L., & Tierz, M. (2019). *Phase transitions and Wilson loops in antisymmetric representations in Chern–Simons-matter theory.* Journal of Physics A: Mathematical and Theoretical, **52(38)**, 385401.
[109] Wadia, S. R. (1980). $N = \infty$ *Phase Transition in a Class of Exactly Soluble Model Lattice Gauge Theories*, Physics Letters B, **93(4)**, 403-410.
[110] Johansson, K. (1998). *The longest increasing subsequence in a random permutation and a unitary random matrix model.* Mathematical Research Letters, **5(1)**, 68-82.
[111] Cunden, F. D., Facchi, P., & Vivo, P. (2015). *Joint statistics of quantum transport in chaotic cavities.* Europhysics Letters, **110(5)**, 50002.
[112] Grabsch, A., & Texier, C. (2015). *Capacitance and charge relaxation resistance of chaotic cavities—joint distribution of two linear statistics in the Laguerre ensemble of random matrices.* Europhysics Letters, **109(5)**, 50004.
[113] Grabsch, A., & Texier, C. (2016). *Distribution of spectral linear statistics on random matrices beyond the large deviation function—Wigner time delay in multichannel disordered wires.* Journal of Physics A: Mathematical and Theoretical, **49(46)**, 465002.
[114] Vivo, P., Majumdar, S. N., & Bohigas, O. (2008). *Distributions of conductance and shot noise and associated phase transitions.* Physical Review Letters, **101(21)**, 216809.
[115] Vivo, P., Majumdar, S. N., & Bohigas, O. (2010). *Probability distributions of linear statistics in chaotic cavities and associated phase transitions.* Physical Review B - Condensed Matter and Materials Physics, **81(10)**, 104202.
[116] Schehr, G., Majumdar, S. N., Comtet, A., & Forrester, P. J. (2013). *Reunion probability of N vicious walkers: typical and large fluctuations for large* N. Journal of Statistical Physics, **150(3)**, 491-530.
[117] Facchi, P., Florio, G., Parisi, G., Pascazio, S., & Yuasa, K. (2013). *Entropy-driven phase transitions of entanglement.* Physical Review A—Atomic, Molecular, and Optical Physics, **87(5)**, 052324.
[118] Nadal, C., Majumdar, S. N., & Vergassola, M. (2010). *Phase transitions in the distribution of bipartite entanglement of a random pure state.* Physical Review Letters, **104(11)**, 110501.
[119] Facchi, P., Marzolino, U., Parisi, G., Pascazio, S., & Scardicchio, A. (2008). *Phase transitions of bipartite entanglement.* Physical Review Letters, **101(5)**, 050502.
[120] De Pasquale, A., Facchi, P., Parisi, G., Pascazio, S., & Scardicchio, A. (2010). *Phase transitions and metastability in the distribution of the bipartite entanglement of a large quantum system.* Physical Review A -Atomic, Molecular, and Optical Physics, **81(5)**, 052324.
[121] Colomo, F., & Pronko, A. G. (2013). *Third-order phase transition in random tilings.* Physical Review E - Statistical, Nonlinear, and Soft Matter Physics, **88(4)**, 042125.
[122] Colomo, F., & Pronko, A. G. (2015). *Thermodynamics of the six-vertex model in an L-shaped domain.* Communications in Mathematical Physics, **339**, 699-728.
[123] Fyodorov, Y. V., & Nadal, C. (2012). *Critical behavior of the number of minima of a random landscape at the glass transition point and the Tracy-Widom distribution.* Physical Review Letters, **109(16)**, 167203.
[124] Krajenbrink, A., & Le Doussal, P. (2019). *Linear statistics and pushed Coulomb gas at the edge of* β*-random matrices: Four paths to large deviations.* Europhysics Letters, **125(2)**, 20009.

[125] Buchanan, M. (2014). *Equivalence principle.* Nature Physics, **10(8)**, 543-543.
[126] Wolchover, N. (2014) *At the Far Ends of a New Universal Law*, Quanta Mag. (2014), `https://lc.cx/Z9ao`.
[127] MacKenzie, R. (2000). *Path integral methods and applications.* Preprint arXiv [quant-ph/0004090].
[128] Rougerie, N. & Serfaty, S. (2016). *Higher-Dimensional Coulomb Gases and Renormalized Energy Functionals.* Communications on Pure and Applied Mathematics, **69(3)**, 519-605.
[129] Sandier, E. & Serfaty, S. (2015). *2D Coulomb gases and the renormalized energy.* The Annals of Probability, **43(4)**, 2026–2083.
[130] Tricomi, F. G. (1951). *On the finite Hilbert transformation.* The Quarterly Journal of Mathematics, **2(1)**, 199-211.
[131] Deift, P. (2000). *Orthogonal Polynomials and Random Matrices: A Riemann-Hilbert Approach*(Vol. **3**). American Mathematical Society.
[132] Saff, E. B., & Totik, V. (2013). *Logarithmic potentials with external fields* (Vol. **316**). Springer Science & Business Media.
[133] Fyodorov, Y. V., Khoruzhenko, B. A., & Simm, N. (2016). *Fractional Brownian motion with Hurst index $H = 0$ and the Gaussian Unitary Ensemble*, Annals of Probability **44(4)**, 2980-3031 (2016).
[134] Garoufalidis, S. and Popescu, I., (2013). *Analyticity of the planar limit of a matrix model.* In Annales Henri Poincaré (Vol. **14**, No. 3, pp. 499-565). Basel: SP Birkhäuser Verlag Basel.